The complete mitogenome of *Arion vulgaris* Moquin-Tandon, 1855 (Gastropoda: Stylommatophora): Mitochondrial genome architecture, evolution and phylogenetic considerations within Stylommatophora

Özgül Doğan [Corresp., 1, 2], **Michael Schrödl** [2, 3, 4], **Zeyuan Chen** [2, 3]

[1] Department of Molecular Biology and Genetics, Faculty of Science, Sivas Cumhuriyet University, Sivas, Turkey

[2] SNSB-Bavarian State Collection of Zoology, Munich, Germany

[3] Department Biology II, Ludwig-Maximilians-Universität, Munich, Germany

[4] GeoBio-Center LMU, Munich, Germany

Corresponding Author: Özgül Doğan
Email address: odogan@cumhuriyet.edu.tr

Stylommatophora is one of the most speciose orders of Gastropoda, including terrestrial snails and slugs, some of which are economically important as human food, agricultural pests, vectors of parasites or due to invasiveness. Despite their great diversity and relevance, the internal phylogeny of Stylommatophora has been debated. To date, only 34 stylommatophoran mitogenomes were sequenced. Here, the complete mitogenome of an invasive pest slug, *Arion vulgaris* Moquin-Tandon, 1855 (Stylommatophora: Arionidae), was sequenced using next generation sequencing, analysed and compared with other stylommatophorans. The mitogenome of *A. vulgaris* measures 14,547 bp and contains 13 protein-coding, two rRNA, 22 tRNA genes, and one control region, with an A+T content of 70.20%. All protein coding genes (PCGs) are initiated with ATN codons except for *COX1* and *ATP8* and all are ended with TAR or T− stop codons. All tRNAs were folded into a clover-leaf secondary structure except for *trnC* and *trnS1* (AGN). Phylogenetic analyses confirmed the position of *A. vulgaris* within the superfamily Arionoidea, recovered a sister group relationship between Arionoidea and Orthalicoidea, and supported monophyly of all currently recognized superfamilies within Stylommatophora. Initial diversification time of the Stylommatophora was estimated as 138.55 million years ago corresponding to Early Cretaceous. The divergence time of *A. vulgaris* and *Arion rufus* (Linnaeus, 1758) was estimated as 15.24 million years ago corresponding to one of Earth's most recent, global warming events, the Mid-Miocene Climatic Optimum. Furthermore, selection analyses were performed to investigate the role of different selective forces shaping stylommatophoran mitogenomes. Although purifying selection is the predominant selective force shaping stylommatophoran mitogenomes, six genes (*ATP8*, *COX1*, *COX3*, *ND3*, *ND4* and *ND6*)

detected by the branch-specific aBSREL approach and three genes (*ATP8*, *CYTB* and *ND4L*) detected by codon-based BEB, FUBAR and MEME approaches were exposed to episodic diversifying selection. The positively selected substitutions mitochondrial PCGs of stylommatophoran species seems to be adaptive to environmental conditions and affecting mitochondrial ATP production or protection from reactive oxygen species effects. Comparative analysis of stylommatophoran mitogenome rearrangements using MLGO revealed conservatism in Stylommatophora; exceptions refer to potential apomorphies for several clades including rearranged orders of *trnW-trnY* and of *trnE-trnQ-rrnS-trnM-trnL2-ATP8-trnN-ATP6-trnR* clusters for the genus *Arion*. Generally, tRNA genes tend to be rearranged and tandem duplication random loss, transitions and inversions are the most basic mechanisms shaping stylommatophoran mitogenomes.

The complete mitogenome of *Arion vulgaris* Moquin-Tandon, 1855 (Gastropoda: Stylommatophora): Mitochondrial genome architecture, evolution and phylogenetic considerations within Stylommatophora

Özgül Doğan[1,2*], Michael Schrödl[2,3,4], Zeyuan Chen[2,3]

[1] Department of Molecular Biology and Genetics, Faculty of Science, Sivas Cumhuriyet University, 58140 Sivas, Turkey.

[2] SNSB-Bavarian State Collection of Zoology, 81247 Munich, Germany.

[3] Department Biology II, Ludwig-Maximilians-Universität, 82152 Planegg-Martinsried, Munich, Germany.

[4] GeoBio-Center LMU, 80333 Munich, Germany.

[*]Corresponding Author:

Özgül Doğan[1,2]

Department of Molecular Biology and Genetics, Faculty of Science, Sivas Cumhuriyet University, 58140 Sivas, Turkey.

Email address: odogan@cumhuriyet.edu.tr

ABSTRACT

Stylommatophora is one of the most speciose orders of Gastropoda, including terrestrial snails and slugs, some of which are economically important as human food, agricultural pests, vectors of parasites or due to invasiveness. Despite their great diversity and relevance, the internal phylogeny of Stylommatophora has been debated. To date, only 34 stylommatophoran mitogenomes were sequenced. Here, the complete mitogenome of an invasive pest slug, *Arion vulgaris* Moquin-Tandon, 1855 (Stylommatophora: Arionidae), was sequenced using next generation sequencing, analysed and compared with other stylommatophorans. The mitogenome of *A. vulgaris* measures 14,547 bp and contains 13 protein-coding, two rRNA, 22 tRNA genes, and one control region, with an A+T content of 70.20%. All protein coding genes (PCGs) are initiated with ATN codons except for *COX1* and *ATP8* and all are ended with TAR or T− stop codons. All tRNAs were folded into a clover-leaf secondary structure except for *trnC* and *trnS1* (AGN). Phylogenetic analyses confirmed the position of *A. vulgaris* within the superfamily Arionoidea, recovered a sister group relationship between Arionoidea and Orthalicoidea, and supported monophyly of all currently recognized superfamilies within Stylommatophora. Initial diversification time of the Stylommatophora was estimated as 138.55 million years ago corresponding to Early Cretaceous. The divergence time of *A. vulgaris* and *Arion rufus* (Linnaeus, 1758) was estimated as 15.24 million years ago corresponding to one of Earth's most recent, global warming events, the Mid-Miocene Climatic Optimum. Furthermore, selection analyses were performed to investigate the role of different selective forces shaping stylommatophoran mitogenomes. Although purifying selection is the predominant selective force shaping stylommatophoran mitogenomes, six genes (*ATP8*, *COX1*, *COX3*, *ND3*, *ND4* and *ND6*) detected by the branch-specific aBSREL approach and three genes (*ATP8*, *CYTB* and *ND4L*) detected by codon-based BEB, FUBAR and MEME approaches were exposed to episodic

diversifying selection. The positively selected substitutions mitochondrial PCGs of stylommatophoran species seems to be adaptive to environmental conditions and affecting mitochondrial ATP production or protection from reactive oxygen species effects. Comparative analysis of stylommatophoran mitogenome rearrangements using MLGO revealed conservatism in Stylommatophora; exceptions refer to potential apomorphies for several clades including rearranged orders of *trnW-trnY* and of *trnE-trnQ-rrnS-trnM-trnL2-ATP8-trnN-ATP6-trnR* clusters for the genus *Arion*. Generally, tRNA genes tend to be rearranged and tandem duplication random loss, transitions and inversions are the most basic mechanisms shaping stylommatophoran mitogenomes.

Keywords: Mollusca, Pulmonate phylogeny, Garden slug, Gene rearrangement, next generation sequencing, positive selection

INTRODUCTION

The Gastropoda is the most speciose class of Mollusca, including snails and slugs with very diverse feeding habits and a wide range of habitats (Barker, 2009). The about 63,000 gastropod species represent 476 families (Bouchet et al., 2017) and radiated in marine, freshwater and terrestrial ecosystems with detritivorous, herbivorous, carnivorous, predatory or parasitic life styles (Ponder & Lindberg, 1997). Most of the terrestrial gastropods are stylommatophoran pulmonates, with approximately 30,000 species distributed from polar to tropical environments. Stylommatophorans are economically important as human food and because of their status of being major agricultural pests and/or vectors of parasites and invasiveness (Barker, 2009). The origin of Stylommatophora is within panpulmonate heterobranchs (Jörger et al., 2010) and the monophyly of the order is undisputed. Internal phylogenetic relationships of stylommatophorans were poorly resolved based on morphology but then investigated molecularly in different sampling sets of taxa with various methods and basically relatively short sequences. Tillier, Masselmot & Tillirt, (1996) used the D2 region of *28S rRNA* to explore the phylogenetic relationships of pulmonates including a few stylommatophoran species, however they reported that these short sequences would not have sufficient resolving power for investigating the relationships owing to the probable rapid radiation of pulmonate species. Wade, Mordan & Clarke, (2001) and Wade, Mordan & Naggs, (2006) presented more comprehensive molecular phylogenies based on relatively longer sequence information of the rRNA gene-cluster using 104 species (Wade, Mordan & Clarke, 2001) and 160 species (Wade, Mordan & Naggs, 2006) from Stylommatophora. Although these phylogenetic reconstructions accurately supported the monophyly of achatinoid and non-achatinoid clades, some clades of families that traditionally have been assumed to be monophyletic and some of the morphological groups based on

excretory system, in particular monophyly of some families and morphological groups were not supported.

The emergence and divergence time of Stylommatophora is also doubtful due to the fragmentary fossil records. The earliest land snails identified as stylommatophoran species are from upper Carboniferous and Permian but their classification has still been controversial (Solem & Yochelson, 1979; Hausdorf, 2000). Bandel, (1991) and Roth et al., (1996) suggested the oldest known fossil records from late Jurassic and Early Cretaceous (*Cheruscicola*) and Early Cretaceous (Pupilloidea). Tillier, Masselmot & Tillirt, (1996) inferred that the Stylommatophora emerged in the transition between late Cretaceous and Paleocene (65-55 Ma) congruent with fossil records, based on the molecular data. However, all of the previous molecular dating analyses on Stylommatophora have been performed either with limited numbers of taxa or molecular markers (Tillier, Masselmot & Tillirt, 1996; Jörger et al., 2010; Dinapoli & Klussmann-Kolb, 2010; Zapata et al., 2014), therefore there is a need for further investigations in a more comprehensive sampling using more markers for better understanding of the phylogeny and timing of evolution of Stylommatophora.

In recent years, there is a rapid increase in the number of sequenced mitochondrial genomes (mitogenomes) in parallel to revolution on high throughput DNA sequencing technology and data mining, providing a powerful tool for phylogenetic analysis (Moritz, Dowling & Brown, 1987; Boore, 1999; Bernt et al., 2013a). Animal mitogenomes are double-stranded circular molecules which are ~16 kb in length and contain 13 protein coding genes (PCGs) forming the respiratory chain complexes: Complex I or NADH: ubiquinone oxidoreductase contains seven subunits of NADH dehydrogenase (*ND1–6* and *ND4L*), complex III or ubiquinol: cytochrome *c* oxidoreductase consists of cytochrome b (CYTB), complex IV or cytochrome *c* oxidase

104 comprises three subunits of cytochrome c oxidase (*COX1–COX3*) and complex V or ATP
105 synthase includes two subunits of the ATPase (*ATP6* and *ATP8*). They also encode the small and
106 large subunit rRNAs (*rrnL* and *rrnS*) and twenty-two tRNA genes for the translation process of
107 PCGs. In general, they harbour a single large non-coding region containing control elements
108 necessary for replication and transcription (Boore, 1999). Mitogenomes have become widely
109 used tools in recent phylogeny, phylogeography and molecular dating analyses in various taxa,
110 because of their (1) relatively small size, (2) the high copy number, (3) maternal inheritance type
111 and (4) relatively rapid rate of evolutionary change (Moritz, Dowling & Brown, 1987; Gray,
112 1989). The sequence information of mitogenomes has also been used in reconstructing
113 phylogenies of several taxonomic groups within/including Gastropoda (White et al., 2011;
114 Stöger & Schrödl, 2013; Sevigny et al., 2015; Uribe et al., 2016a,b; Romero, Weigand &
115 Pfenninger, 2016; Yang et al., 2019). Although there have been some criticisms about the usage
116 of mitogenomes in construction of gastropod phylogeny because of long branch attraction,
117 substitution saturation and strand-specific skew bias (Stöger & Schrödl, 2013), within the
118 recently diversified lineages of gastropods, the use of mitogenomes resulted in highly resolved
119 phylogenies (Williams, Foster & Littlewood, 2014; Osca, Templado & Zardoya, 2014). Besides
120 the use of the mitogenome in sequence-based phylogenies, mitogenome rearrangements can also
121 provide phylogenetic signals (Grande, Templado & Zardoya, 2008; Stöger & Schrödl, 2013; Xie
122 et al., 2019b). Although the mitogenome is widely used in phylogeny of many gastropod groups,
123 there are limited numbers of reported stylommatophoran mitogenomes and phylogenetic studies
124 in Stylommatophora in terms of usage of mitogenome sequence and rearrangement (Romero,
125 Weigand & Pfenninger, 2016; Xie et al., 2019a; Yang et al., 2019). To date, complete or nearly

126 complete mitogenomes have been reported for only 34 stylommatophoran species (NCBI,
127 September, 2019).

128 In this study, we sequenced and annotated the complete mitogenome of *Arion vulgaris* Moquin-
129 Tandon, 1855 (Stylommatophora: Gastropoda), which is considered as a serious invasive pest
130 both in agriculture and private gardens. We compared it with the mitogenome of its congener
131 *Arion rufus* (Linnaeus, 1758), and with all other previously reported stylommatophoran
132 mitogenomes. We also reconstructed a phylogeny from stylommatophoran mitogenomes to
133 estimate the phylogenetic position of *A. vulgaris* and to test the informativeness of mitogenome
134 data in the reconstruction of Stylommatophora phylogeny. In addition, we obtained a dated
135 phylogeny using this mitogenome dataset and fossil calibrations to estimate divergence times
136 within Stylommatophora. Furthermore, selection analyses were performed to investigate the role
137 of different selective forces shaping stylommatophoran mitogenomes. Finally, we compared the
138 mitogenome organisations of stylommatophoran species using a comparative and phylogeny
139 based method and tried to uncover the evolutionary pathways of mitogenome rearrangements.

140

141 **MATERIALS AND METHODS**

142 **Specimen collection and DNA extraction**

143 The specimen of *A. vulgaris* was collected from the garden of the Zoologische Staatssammlung
144 München (ZSM), Germany. Total genomic DNA was extracted from body muscle using CTAB
145 method (Doyle & Doyle, 1987).

146

147 **Mitogenome sequencing, annotation and analyses**

148 The whole-genome sequencing was conducted with 150 bp pair-end reads on the Illumina
149 Hiseq4000 Platform (Illumina, San Diego, CA) using 350 bp insert size libraries. Raw reads
150 were processed by removing low quality reads, adapter sequences and possible contaminated
151 reads using Fastp v0.20.0 (Chen et al., 2018) and Lighter v1.0.7 (Song, Florea & Langmead,
152 2014). In total, about 7.5G high quality base pairs of sequence data were obtained and the
153 mitogenome was assembled using the MitoZ software (Meng et al., 2019), followed by manual
154 curation using Geneious R9 (Kearse et al., 2012).

155 The annotation of tRNA genes of the *A. vulgaris* mitogenome was performed using MITOS
156 (http://mitos.bioinf.uni-leipzig.de/index.py) (Bernt et al., 2013b) and ARWEN web servers
157 (Laslett & Canbäck, 2008) based on their secondary structures and anticodon sequences. The
158 locations and boundaries of PCGs and rRNA genes were identified manually by comparing with
159 the *A. rufus* (KT626607) homologous gene sequences. The visualization of the secondary
160 structure of tRNA genes was performed using VARNA v3-93 (Darty, Denise & Ponty, 2009)
161 and RNAviz 2.0.3 (De Rijk, Wuyts & De Wachter, 2003). Intergenic spacers and overlapping
162 regions between genes were estimated manually. The largest non-coding region was defined as
163 control region and the Mfold server (Zuker, 2003) was used to predict the secondary structure of
164 this region. The “palindrome” tool within the European Molecular Biology Open Software Suite
165 (EMBOSS) (Rice, Longden & Bleasby, 2000) was used for searching the palindromic sequences
166 in the control region. Finally, the complete mitogenome of *A. vulgaris* has been deposited in
167 GenBank (pending accession number). The mitogenome of *A. vulgaris* is visualized using
168 OrganellarGenomeDRAW (OGDRAW) (Greiner, Lehwark & Bock, 2019).

169 The nucleotide compositions, average nucleotide and amino acid sequence divergences and the
170 relative synonymous codon usages (RSCU) of PCGs were computed using MEGA v7.0 (Kumar,
171 Stecher & Tamura, 2016). The strand asymmetries were calculated according to the following
172 formulas: AT-skew = [A − T] / [A + T] and GC-skew = [G − C] / [G + C] (Perna & Kocher,
173 1995).

174

175 **Phylogenetic and comparative analyses**

176 *Alignment and model selection*

177 Phylogenetic and comparative analyses were performed using the mitogenome dataset of 34
178 stylommatophoran species representing 18 families, and using one species from
179 Systellommatophora, one species from Hygrophila, and one species from Ellobioidea as
180 outgroups (Table 1). Each tRNA and rRNA gene was aligned individually using MAFFT (Katoh
181 & Standley, 2013) algorithm in Geneious R9 (Kearse et al., 2012). The alignment of nucleotide
182 sequences of each PCG was performed using MAFFT algorithm and the "translation align"
183 option implemented in Geneious R9. The final alignment files were then concatenated using
184 SequenceMatrix v.1.7.8 (Vaidya, Lohman & Meier, 2011). The optimal partitioning scheme and
185 substitution models were inferred by PartitionFinder v1.1.1 (Lanfear et al., 2012) using the
186 Bayesian Information Criterion and the "greedy" algorithm with the option of "unlinked" branch
187 lengths. The best-fit partitioning scheme and nucleotide substitution models were used in
188 phylogenetic analyses (Table S1).

189

Assessing the substitution saturation level

The substitution saturation levels in different genes and codon positions were estimated comparing the uncorrected p-distances and the distances calculated by applying the GTR + G + I evolutionary model selected by the jModelTest v2.1.7 (Darriba et al., 2012). All distances were computed with PAUP v4.0 b10 (Swofford, 2002).

Phylogenetic reconstruction

Two different datasets were created for phylogenetic analyses to test the influence of saturated genes and codon positions: (1) 13 PCGs including all codon positions plus the 22 tRNAs and two rRNAs (P123RNA) and (2) PCGs excluding the five saturated genes and third codon positions, plus 22 tRNAs and two rRNAs (8P12RNA, Table S2). Maximum likelihood (ML) trees were constructed with RAxML v8.0.9 (Stamatakis, 2014) implemented in Geneious R9 applying the best-fit evolutionary model for each partition under 1000 bootstrap replicates. For Bayesian Inference (BI) analyses, MrBayes v3.2.2 (Ronquist et al., 2012) was employed with two independent runs of 10 million generations with four Markov chains (three cold, one heated), sampling every 1000 generations and a burn-in of 25% trees. The stationarity of the chains was assessed using the program Tracer v1.7 (Rambaut et al., 2018). The consensus phylogenetic trees were visualized using FigTree v1.4.0 (Rambaut, 2012).

Divergence time estimation

MCMCTree program implemented in the Phylogenetic Analysis by Maximum Likelihood (PAML) package v4.9 (Yang, 2007) was used for Bayesian estimation of divergence times of each species. Substitution rate per site was estimated by BASEML and was used to set the prior

for the mean substitution rate in the Bayesian analysis. MCMC was run by 50 × 10000 iterations with the REV substitution model. The soft bounds of *Helix pomatia* + *Helix aspersa* (divergence time between 34 MY and 42 MY), (*Aegista aubryana* + (*Aegista diversifamilia* + (*Dolicheulota formosensis* + *Mastigeulota kiangsinensis*))) (divergence time between 25 MY and 51 MY), and *Camaena cicatricose* + *Camaena poyuensis* (divergence time between 16 MY and 39 MY) as external calibration (Razkin et al., 2015) and the fossil Tectipleura calibration of 244 (210–279) million years ago (Ma) for the root (Kano et al., 2016).

Selection analyses

The CODEML implemented in PAML was used to estimate the ratio of nonsynonymous/synonymous substitution rate (ω=dN/dS) and to explore the role of different selective constraints working on each PCG under the one-ratio model (Model A: model=0, NSsites=0, fix_omega=0, omega= 1). Gaps and ambiguous sites of sequence alignments were included in the analyses. For each PCG, likelihood ratio tests (LRTs) were used to compare the null neutral model (Model B: model = 2, NSsites = 2, fix_omega = 1, omega = 1) against alternative models of branch-specific positive selection (Model C: model=2, NSsites=2, fix_omega=0, omega= 1.5). The Bayes Empirical Bayes (BEB) algorithm in CODEML was used to detect the positively selected sites. Furthermore, the adaptive branch-site random effects likelihood (aBSREL) (Smith et al., 2015) implemented in DATAMONKEY webserver (Weaver et al., 2018) was used to search the signatures of episodic positive diversifying selection testing each branch. In addition, mixed effects model of evolution (MEME) (Murrell et al., 2012) was used to detect episodic or diversifying selection at individual sites and a fast, unconstrained Bayesian approximation for inferring selection (FUBAR) (Murrell et al., 2013) was used for

236 providing additional support to the detection of sites evolving under positive or negative
237 selection. Each PCG was also evaluated in terms of properties and magnitude of amino acid
238 changes using TreeSAAP v3.2 (Woolley et al., 2003), which uses 31 properties of amino acids
239 and categorizes the degree of substitutions to eight categories (1−8).

240

241 *Comparison of mitogenome organizations*

242 Mitogenome organizations and gene rearrangements of stylommatophoran species were analysed
243 via the CREx web server (http://pacosy.informatik.uni-leipzig.de/crex) (Bernt et al., 2007). The
244 gene orders of ancestral nodes were reconstructed using the Maximum Likelihood for Gene
245 Order Analysis (MLGO, http://geneorder.org/) (Hu, Lin & Tang, 2014) with the input tree
246 obtained by phylogenetic approaches, and the orders of the protein coding, rRNA and tRNA
247 genes were compared with the inferred ancestral mitogenomes. A distance matrix was calculated
248 based on number of common intervals, and the output diagram visually examined to identify
249 shared and/or derived gene rearrangements as well as mechanisms of rearrangements.

250

251 **RESULTS AND DISCUSSION**

252 **Mitogenome characteristics and nucleotide composition**

253 The complete mitogenome sequence of *A. vulgaris* was obtained with a length of 14,547 bp
254 (Table 2) and its size was within the range of the those of other reported stylommatophoran
255 mitogenomes, varying between 13,797 bp in *C. poyuensis* and 16,879 bp in *Partulina redfieldi*
256 (Price et al., 2018). It includes the entire set of 37 mitochondrial genes: 13 PCGs, 22 tRNAs and
257 two rRNAs. Twenty-four genes were located on the J strand, while the remainings were encoded
258 by the opposite N strand (Table 2, Fig. 1).

The nucleotide composition of *A. vulgaris* mitogenome was distinctly biased towards A and T, with a 70.20% A+T content, and comparable to other reported stylommatophoran mitogenomes, varying between 59.79% A+T in *Cepea nemoralis* (Yamazaki et al., 1997) and 80.07% A+T in *Achatinella mustelina* (Price et al., 2016a) (Tables 3 and S3). A bias towards A and T nucleotides was also observed in PCGs of the *A. vulgaris* mitogenome with a 69.34% A+T content (Table 3). The A+T content of the 3rd codon position (79.64%) was higher than those of the 2nd (64.21%) and 1st codon positions (64.18%). Similar to other reported stylommatophoran mitogenomes (Table S3), the AT− and GC−skews were found slightly negative (−0.0756) and positive (0.0431) in the whole mitogenome of *A. vulgaris*, respectively. A pronounced T and G skew was also observed in all PCGs (−0.1508, 0.0472), PCGs on the majority strand (−0.1447, 0.0596), and tRNA genes (−0.0010, 0.1582) (Table 3). The T− and G−skewed mitogenome of *A. vulgaris* might be explained by the spontaneous deamination of cytosine during replication and transcription processes (Reyes et al., 1998). The PCGs encoded on the minority strand displayed a T− and C− skewed pattern (−0.1783 AT−skew, −0.0065 GC−skew), contrary to the expected high rates of Ts and Gs on the minority strand for most of the metazoans (Hassanin, Léger & Deutsch, 2005).

Protein coding genes and codon usage

Compared with the mitogenome of *A. rufus*, the lengths of PCGs of *A. vulgaris* were distinct except for *COX1*, *COX2*, *CYTB* and *ND1* genes. The *ND6* gene was the most variable gene in length and was longer in the *A. vulgaris* mitogenome by 11 codons. The most conserved PCG was *COX1* (97.26%) whereas the least conserved was *ATP8* (58.21%) based on the amino acid identities between the two *Arion* mitogenomes.

In the *A. vulgaris* mitogenome, most of the PCGs initiated with typical ATN start codon, except for *COX1*, *ND5* and *ATP8* genes which use TTG, ACA and GTG triplets as start codons, respectively (Table 2). Most of the PCGs were inferred to use TAR as termination codon, except for *ND4L* and *COX3* which have an abbreviated T− termination codon and their products are probably completed via post-transcriptional polyadenylation (Anderson et al., 1981; Ojala, Montoya & Attardi, 1981).

The most frequently used amino acids by the PCGs of the mitogenome of *A. vulgaris* were leucine (16.71%), serine (10.33%) and phenylalanine (7.69%), similar to PCGs of the mitogenome of *A. rufus* (Leu 15.91%, Ser 10.18%, Phe 7.73%). The codons rich in A and T, such as UUA−Leu, AUU−Ile, UUU−Phe, AUA−Met, UAU−Tyr, were the most frequently used codons. The codons rich in terms of G and C content, CGC− CGG−Arg, CAG−Gln, UGC−Cys, CUC−Leu and UCG−Ser were rarely used in both *Arion* mitogenomes (Table S4, Fig. 2), and reflected a significant relationship between codon usage and nucleotide content.

tRNA and rRNA genes

All of the tRNA genes could be folded into a usual clover-leaf secondary structure, except for *trnS1* (AGN) and *trnC* which lacked dihydrouridine (DHU) and TΨC arms, respectively and formed simple loops (Fig. S1). Their lengths ranged between 57 bp (*trnC*) and 78 bp (*trnG*), with an average 72.72% A + T content. 26 mismatched positions were observed in stem regions and all of the mismatches were G-U pairs (Fig. S1).

The exact boundaries of rRNA genes were determined as being bounded by the adjacent tRNA genes. The *rrnL* gene was located between *trnV* and *trnL1* genes, and the *rrnS* gene was located between *trnQ* and *trnM* genes. The length of the *rrnL* gene was 1013 bp, with a 71.17% A + T

content, while that of *rrnS* gene was 747 bp, with a 71.75% A + T content. These were comparable in ranges to homologous genes in other reported stylommatophoran species, ranging from 605 to 1215 bp in *rrnL* and from 564 to 857 bp in *rrnS.*

Non-coding and overlapping regions

The total length of intergenic regions in the *A. vulgaris* mitogenome was 670 bp in 16 locations ranging between 1 and 370 bp (Table 2). In general, the largest non-coding region in the animal mitogenomes is considered to contain the signals for replication and transcription, and so called as the control region (Wolstenholme, 1992). The possible candidate for the control region in *A. vulgaris* mitogenome was the largest non-coding region located between *trnY* and *trnG genes* with 370 bp in length. This sequence did not give BLAST hits with other putative CRs of other molluscan mitogenomes, however a part of the sequence with 67 bp in length displayed 79.11% sequence similarity with the mitochondrial control region of an amphibian species (*Indotyphlus maharashtraensis,* KF540157). Nucleotide composition of this region was slightly biased towards A + T with a 69.73% A + T content. The putative control region had a nine bp poly-T stretch and formed a stable secondary structure comprising seven stems and loops (Fig. 3). Furthermore, this sequence also contained a lot of palindromic sequences which are varying between 4 and 8 bp, but tandemly repeated sequences were not found.

The second largest non-coding region was found between *trnW* and *trnY* with a length of 91 bp (Table 2). The A + T composition of the sequence was higher than that of whole genome and putative control region with an 86.81% A + T. This non-coding region also contained a seven bp poly-A stretch and was folded into a secondary structure with two stem and loops. This

secondary structure forming AT-rich sequence might function as the origin of the second strand (Wolstenholme, 1992).

Eleven overlapping regions with a total length of 164 bp were found throughout the mitogenome of *A. vulgaris*. The largest overlapping region was 41 bp in length and located between *ND6* and *ND5* genes, while the second largest was 32 bp and located between *trnL2* and *ATP8* (Table 2).

Phylogeny and divergence times of stylommatophoran species

Regression analyses of pairwise distances revealed that the 1st and 2nd codon positions of *ATP8*, *ND2*, *ND3*, *ND4L* and *ND6* genes, as well as the 3rd codon positions of all PCGs were saturated (Table S2). Four phylogenetic reconstruction analyses were performed with combination of inference methods and different data matrices to test the influence of inference methods and saturation level of genes/codon positions on tree topology and nodal support. Three different tree topologies were obtained as the results of these analyses, and topologies were sensitive to both inference methods and exclusion of saturated genes/ codon positions (Figures 4 and S2-4). Nodal support values were always higher in BI trees than ML trees of the corresponding dataset. A highly resolved tree with higher nodal support values was obtained from the BI approach of the dataset 8P12RNA, and hence considered as most reliable tree for discussion.

The tree confirmed the taxonomic position of *A. vulgaris* as sister to *A. rufus* and recovered the monophyly of the Arionoidea superfamily (Arionidea + Philomycidae) with high support values [posterior probability (PP)=1.00]. A well-supported sister group relationship between Arionoidea and Orthalicoidea has been recovered (PP=0.98) for the first time. However, sister group relationships between Arionoidea and Succineoidea (Xie et al., 2019b), and Limacoidea (Wade, Mordan & Naggs, 2006; Holznagel, Colgan & Lydeard, 2010), and Limacoidea + (Succineoidea

350 + Helicoidea) (Dayrat et al., 2011), and Urocoptoidea + Enoidea + Helicoidea (Jörger et al.,
351 2010), or Helicoidea + Urocoptoidea (Yang et al., 2019) were reported by previous studies.

352 The monophyly of all included families and superfamilies were also supported with high support
353 values (Fig. 4). Arionoidea + Orthalicoidea clade was recovered as sister group to Succineoidea
354 + (Urocoptoidea + (Polygyroidea + Helicoidea)). The tree (Fig. 4) also recovered *Deroceras*
355 *reticulatum* (Agriolimacidae: Limacoidea) at the most basal placement and did not support the
356 monophyly of the suborder Helicina similar to the tree in Yang et al. (2019).

357 A chronogram for Stylommatophora divergence times based on the obtained tree topology is
358 shown in Figure 5. According to our divergence time analysis, the crown age of
359 stylommatophorans was estimated as 138.55 Ma (180.8−107.4 Ma, 95% CI) corresponding to
360 Early Cretaceous. Our estimated times for initial diversification of Stylommatophora are slightly
361 older but broadly congruent with the fossil records and previous studies (Tillier, Masselmot &
362 Tillirt, 1996; Jörger et al., 2010; Dinapoli & Klussmann-Kolb, 2010). Although Solem &
363 Yochelson, (1979) suggested a Paleozoic origin for Stylommatophora, the widely accepted fossil
364 records with recognizable taxa began from Late Cretaceous (Bandel & Riedel, 1994). The
365 Cretaceous origin of stylommatophoran species was also suggested by sequence studies of 28S
366 rDNA fragments by Tillier, Masselmot & Tillirt, (1996), of combined data of 18S, 28S, 16S
367 rDNA and COI by Dinapoli & Klussmann-Kolb, (2010) and Jörger et al., (2010). The
368 diversification of the stylommatophoran species may have been influenced by the explosive
369 radiation of angiosperms and speciation by host-switching during Cretaceous (Friis, Pedersen &
370 Crane, 2010).

371 The split time of *Achatina fulica* from other stylommatophoran species was inferred as 131.91
372 Ma in Early Cretaceous. The splits of the superfamilies Orthalicoidea and Arionoidea, of

373 Succineoidea from Urocoptoidea + (Polygyroidea + Helicoidea), and of Clausilioidea +
374 (Pupilloidea + Achatinelloidea) were dated to 114.18 Ma (148.7-87.2 Ma, 95% CI), 113.30 Ma
375 (146.1-87.9 Ma, 95% CI) and 111.88 Ma (148.1-84.2 Ma, 95% CI), respectively, coinciding to
376 the beginning of the Albian (Early Cretaceous). The crown ages of the superfamilies Arionoidea,
377 Urocoptoidea, Helicoidea and Pupilloidea were estimated corresponding to Late Cretaceous
378 (84.82, 75.23, 74.39 and 70.06 Ma, respectively). The split of the two *Arion* species and the
379 crown age of Achatinelloidea species were dated to 15.24 Ma (30.0-7.6 Ma, 95% CI) and 13.01
380 Ma (19.7-8.2 Ma, 95% CI), respectively, corresponding to the Miocene. The divergence time of
381 *A. vulgaris* and *A. rufus* corresponds to one of Earth's most recent, global warming events, the
382 Mid-Miocene Climatic Optimum (MMCO, 17-14.75 Ma) (Böhme, 2003). The MMCO is
383 thought to have contributed to floristic and faunistic diversity across the world and so to animal-
384 plant interactions, correlating with the rise in temperature (Barnosky & Carrasco, 2002; Vicentini
385 et al., 2008; Tolley, Chase & Forest, 2008). The change of plant diversity, emergence of new
386 host plants and the relative warm period may have triggered the diversification of *Arion* species.
387 The divergence time of two polygyroid species was inferred as 0.45 Ma (1.1-0.1 Ma, 95% CI), in
388 the Pleistocene.

389

390 **Selective pressures on stylommatophoran mitogenomes**

391 The ω value for each of the 13 PCGs was inferred under one-ratio model using PAML and
392 presented in Table 4. All of the ω values were extremely low (ω<1), ranging between 0.0129 for
393 *COX1* and 0.2198 for *ATP8,* reflecting that all genes were under strong purifying selection
394 consistent with the general mitogenome evolution pattern in animals (Rand, 2001; Bazin, Glemin
395 & Galtier, 2006). Although purifying selection is the predominant selective force shaping

396 stylommatophoran mitogenomes, the comparison of the null neutral model and alternative
397 branch-specific positive selection model revealed six of the PCGs (*ATP6*, *COX2*, *COX3*, *ND2*,
398 *ND4* and *ND5*) have variation in ω values along different branches. The variability in ω values
399 indicated different selective forces acting on each gene as well as each branch. A more sensitive
400 branch-site method, aBSREL, providing three states for each branch and allowing each site to
401 evolve under any kind of the value (<1, 1 or >1) (Smith et al., 2015), was used for evaluating and
402 confirming the selective forces across lineages determined by PAML analysis. All of the
403 branches in the stylommatophoran phylogeny tested with this analysis for each PCG and the
404 episodic diversifying selection detected genes were different from the results of branch-site
405 model of PAML (Table 5) except for *COX3* and *ND4*. The aBSREL analyses discovered
406 episodic diversifying selection in *ATP8* (at the branch leading to *Microceramus. pontificus*),
407 *COX1* (at the branch leading to *A. mustelina*), *COX3* (at the branch leading to Arionoidea and the
408 branch leading to *Philomycus bilineatus*), *ND3* (at the branch leading to *Helicella itala*), *ND4* (at
409 the branch leading to *Succinea putris*) and *ND6* (at the branch leading to *Vertigo pusilla*). Due to
410 their important function, mitochondrial genes might have a few positively selected sites and the
411 signatures of purifying selection likely mask those of positive selection (Meiklejohn, Montooth
412 & Rand, 2007; da Fonseca et al., 2008). Therefore, two different methods were used to detect
413 positive selection in addition to BEB analysis: FUBAR which estimates the rates of
414 nonsynonymous and synonymous substitutions at each codon in a phylogeny, and MEME which
415 estimates the probability for a codon to have experienced episodic positive selection and allows
416 the ω ratio to vary across branches and codons. BEB analysis identified eight positively selected
417 codons in total in three genes (*ND2*, *ND4* and *ND5*), whereas FUBAR defined six positively
418 selected codons in five genes (*ATP6*, *ATP8*, *COX2*, *CYTB* and *ND4L*). The MEME analysis

found the signals of episodic positive selection at 22 codons in nine genes (*ATP6*, *ATP8*, *CYTB*, *ND2-6*, and *ND4L*). There was not any shared codon determined by all of the three analyses (Table 6). Only four codons in three genes were shared by the results of FUBAR and MEME analyses: 44th codon in *ATP8* gene, 12th codon in *CYTB* gene, and 13th and 57th codons in *ND4L* gene. Therefore, we focused only on these four codons in the TreeSAAP analyses. The positively selected substitution at codon 44 in *ATP8* gene was the change of TTA (Leu) to ATT (Ile) at branches leading to *M. kiangsinensis*, *Cerion incanum* and *Cerion uva*. This substitution was a radical chemical change with a magnitude category of 8 and had an impact on the increment of the equilibrium constant (ionization of COOH). The change at the codon 12 in *CYTB* gene was a conserved change with a magnitude category of 1 and was a substitution of TTG (Leu) to ATG (Met). The positively selected substitutions in *ND4L* gene were the change of ATT (Ile) to ATA (Met) at branch leading to *H. pomatia*, to GTT (Val) at branch leading to *C. nemoralis* at codon 13, and the change of TTT (Phe) to AAT (Asn) at branch leading to Arionidae family at codon 57. The substitution at the 13th codon was a radical change with a magnitude category of 8 altering the equilibrium constant (ionization of COOH), while that at the 57th codon was a radical change with a magnitude category of 7 and modifying the solvent accessibility of the protein.

Consequently, six positive selected genes (*ATP8*, *COX1*, *COX3*, *ND3*, *ND4* and *ND6*) detected by branch-specific aBSREL approach and three genes (*ATP8*, *CYTB* and *ND4L*) detected by codon-based BEB, FUBAR and MEME approaches were exposed to episodic diversifying selection. Four of these genes (*ND3*, *ND4*, *ND4L* and *ND6*) play an important role in oxidative phosphorylation and are subunits of NADH dehydrogenase (Complex I) which is the most complicated and largest proton pump of the respiratory chain coupling electron transfer from

NADH to ubiquinone. In addition to its important role in energy production, it has been shown that complex I is implicated in the regulation of reactive oxygen species (ROS) (Sharma, Lu & Bai, 2009). Substitutions in this complex might have been favoured for increasing the efficiency of proton pumping or regulating the response to ROS depending varying amount of oxygen in the atmosphere and adaptation to conditions in new habitats (temperature, humidity, altitude) and / or hosts. *CYTB* gene encodes only mitogenome derived subunit of Complex III and catalyses reversible electron transfer from ubiquinol to cytochrome c (da Fonseca et al., 2008). The positively selected sites in complexes I and III have been suggested to contribute to environmental adaptation in different groups such as mammals, birds, fishes and insects (da Fonseca et al., 2008; Garvin, Bielawski & Gharrett, 2011; Garvin et al., 2014; Melo-Ferreira et al., 2014; Morales et al., 2015; Li et al., 2018). In the cytochrome *c* oxidase complex (Complex IV), *COX1* protein catalyses electron transfer to the molecular oxygen; *COX2* and *COX3* belong to the catalytic core of the complex may act as a regulator. *ATP8* gene encodes the part of ATP synthase (Complex V) regulating the assembly of complex (da Fonseca et al., 2008). The favoured substitutions in *COX3* and *ATP8* gene might have an impact on assembly of the complexes IV and V. The positively selected substitutions and random accumulation of variation in mitochondrial PCGs of stylommatophoran species thus seem to be adaptive and affecting mitochondrial ATP production or protection from ROS effects, however effects of substitutions should be examined in a larger sample by considering protein folding and three-dimensional structure of complexes.

Gene rearrangements in stylommatophoran mitogenomes

The ancestral mitogenome organisation of each node in the phylogeny was inferred using the maximum likelihood approach. The organisation of the hypothetical ancestral Stylommatophora mitogenome (node: A34, Fig. 4) was identical with that of *D. reticulatum* as well as those of *Albinaria caerulea*, *Cernuella virgata* and *H. itala*. The mitogenome of *A. fulica* has only experienced the transposition of *trnP* to the downstream of *trnA* compared to its most recent ancestral mitogenome organisation. The common ancestors of Clausilioidea + (Pupilloidea + Achatinelloidea) (node: A31, Fig. 4), Orthalicoidea + Arionoidea (node: A22, Fig. 4), and Succineoidea + (Urocoptoidea + (Polygyroidea + Helicoidea)) (node: A18, Fig. 4) maintained the same order of hypothetical ancestral stylommatophoran mitogenome. In the mitogenome of the most recent common ancestor (MRCA) of Pupilloidea + Achatinelloidea (node: A30, Fig. 4), the reversal of *trnW*, *trnG* and *trnH* genes occurred individually and were followed by the reversal of the cluster *trnW-trnG-trnH*. In the superfamily Pupilloidea, rearrangements of several tRNA genes were observed: the transposition of the cluster *trnD-trnC* to downstream of *trnW* in *Pupilla muscorum*, transpositions of cluster *trnH-trnG* to downstream of *trnW* and of *trnT* to upstream of *COX3* in *Orcula dolium*, transposition of *trnG* to downstream of *trnW* in *V. pusilla* and the reversal of *trnQ* in *Gastrocopta cristata*. In the mitogenome of the MRCA of the superfamily Achatinelloidea (node: A26, Fig. 4), *trnF-COX2-trnY-trnH-trnG-trnW-*<u>*trnQ*</u>*-*<u>*ATP8*</u>*-*<u>*trnN*</u>*-*<u>*ATP6*</u>*-*<u>*trnR*</u>*-*<u>*trnE*</u>*-*<u>*rrnS*</u>*-*<u>*trnM*</u> gene cluster rearranged as *trnW-*<u>*trnQ*</u>*-*<u>*ATP8*</u>*-*<u>*ATP6*</u>*-*<u>*trnR*</u>*-*<u>*trnE*</u>*-*<u>*rrnS*</u>*-*<u>*trnM*</u>*-trnF-COX2-trnY-trnH-trnG-*<u>*trnN*</u> via tandem duplication random loss (TDRL) mechanism. The organisation of the mitogenomes of achatinelloid species nearly matched with the putative ancestral order, except for *Achatinella sowerbyana* which has a transposed position of *trnK* to downstream of *ATP8* and a second copy of *trnL2*, and for *P. redfieldi* which has the inversion of *trnE* and *trnN* genes.

The mitogenome of *Naesiotus nux* has almost the same organisation with its MRCA (node: A22, Fig. 4), except for the second inverted copy of *ND4L* located between *trnL1* and *trnP*. The MRCA of the superfamily Arionoidea (node: A21, Fig. 4) had also identical mitogenome organisation with the ancestor of Stylommatophora, and the MRCAs of the families Arionidae (node: A19, Fig. 4) and of Philomycidae (node: A20, Fig. 4) were derived from this ancestor. The mitogenome of node A19 had shuffled positions of *trnY* and *trnW*, and also transpositions of *trnE* to downstream of *trnQ* and of *rrnS*-*trnM* to upstream of *trnQ*. Both *Arion* mitogenomes also shared this mitogenome organisation and the rearranged orders of *trnW-trnY* and *trnE-trnQ-rrnS-trnM-trnL2-ATP8-trnN-ATP6-trnR* clusters seem to be synapomorphies of this genus. The mitogenome organisation of the node A20 was quite different from those of other stylommatophoran species, which had rearranged positions of almost all genes between *COX1* and *trnI* via two-steps TDRL, and two Philomycidae species also had identical organisation except for *P. bilineatus* had a second copy of *trnC* located downstream of the original copy.

The mitogenome of *S. putris* has experienced the transpositions of *trnF* to upstream of *trnD* and of *trnW* to upstream of *trnY*, and also reverse transposition of the cluster *trnW-trnY* to the upstream of *ND3*. The MRCA of the all urocoptoid species (node: A16, Fig. 4) only had the reversal of *trnQ* gene from minor to major strand and *M. pontificus* has also maintained the identical arrangement. The four step requiring rearranged gene cluster was identified in the mitogenome of the MRCA of the genus *Cerion* (node: A15, Fig. 4): (i) reversal of *trnV-rrnL-trnL1*, (ii) reversal of *trnP*, (iii) reversal of *trnA*, and (iv) reversal of the cluster *trnL1-rrnL-trnV-trnP-trnA*. The mitogenome organisation remained the same in all three *Cerion* species and the rearranged state of *trnA-trnP-trnV-rrnL-trnL1* cluster might be a synapomorphy for this genus.

The MRCAs of the polygroid species (node: A12, Fig. 4) and Camaenidae + Bradybaenidae (node: A5, Fig. 4), as well as the *Polygyra cereolus* and *Praticolella mexicana,* had the transposed position of *trnG-trnH* to the upstream of *trnY*. The rearrangement of this cluster as *trnG-trnH-trnY* could be suggested as a synapomorphy for Polygyroidea, but more sampling is required to confirm its status at superfamily level. In the superfamily Helicoidea, the MRCAs of Geomitridae (node: A9, Fig. 4) and Geomitridae + Helicidae (node: A10, Fig. 4) shared the identical mitogenome organisation with the MRCA of Stylommatophora. Both of the Geomitridiae species had also same mitogenome organisation except for *ATP8* in *C. virgata,* in which this gene was missing, however it seems to be likely a misannotation. The mitogenome of MRCA of Helicidae species (node: A8, Fig. 4) had experienced the transpositions of *trnP* and cluster *trnT*-*COX3* to downstream of *ND6* and to upstream of *trnS1*, respectively. The mitogenome organisations of two *Helix* species and *C. nemoralis* have not changed and *trnA-ND6-trnP* and *trnS2-trnT-COX3-trnS1* gene orders might be interpreted as synapomorphic for these three species. However, the individual reversals of *trnA*, *ND6* and *trnP* genes followed by reversal of the cluster *trnA*-*ND6*-*trnP*, and reversal of *trnS1* were observed in *Cylindrus obtusus* mitogenome. In the mitogenomes of the species of the family Camaenidae, only the transpositions of *trnD* and *trnY* to downstream of *COX2* and to upstream of *trnG* were found, respectively. The arrangement of the *trnC-trnF-COX2-trnD-trnY-trnG* cluster could be considered as a synapomorphy for camaenid species, however the taxonomic level of this synapomorphy need to be evaluated in a wider taxonomic range. In the family of Bradybaenidae, the MRCA mitogenome had experienced only the reversal of *trnW.* In addition to this rearrangement, *Aegista* species also have the transposition of *ND3* gene to the downstream of

trnW and the rearranged position of *ND3-trnW* cluster appears to be a synapomorphy for the genus.

CONCLUSIONS

The sequencing and annotation of the mitogenome of *A. vulgaris* and its comparison with other stylommatophoran mitogenomes allow us to denote several conclusions: (i) the mitogenome characteristics of *A. vulgaris* are mostly consistent with the reported stylommatophoran mitogenomes, (ii) rearrangement events are detected in the *trnW-trnY* and *trnE-trnQ-rrnS-trnM-trnL2-ATP8-trnN-ATP6-trnR* gene clusters which may be apomorphic for the genus *Arion*, but further investigations are necessary, (iii) stylommatophoran mitogenome sequence information without the saturated positions seems to be useful for reconstructing phylogeny and estimating divergence times, and the taxon set used should be expanded, (iv) although purifying selection is the dominant force in shaping the stylommatophoran mitogenomes, in the background, several codons or different branches have experienced episodic diversifying selection suggesting adaptation to new environmental conditions.

ACKNOWLEDGMENTS

This study has received funding from the European Union's Horizon 2020 research and innovation programme under the Marie Skłodowska-Curie grant agreement No 764840.

REFERENCES

Ahn S-J., Martin R., Rao S., Choi M-Y. 2017. The complete mitochondrial genome of the gray garden slug *Deroceras reticulatum* (Gastropoda: Pulmonata: Stylommatophora). *Mitochondrial DNA Part B* 2:255–256. DOI: 10.1080/23802359.2017.1318677.

Anderson S., Bankier AT., Barrell BG., De Bruijn MHL., Coulson AR., Drouin J., Eperon IC., Nierlich DP., Roe BA., Sanger F., Schreier PH., Smith AJH., Staden R., Young IG. 1981. Sequence and organization of the human mitochondrial genome. *Nature* 290:457–465. DOI: 10.1038/290457a0.

Bandel K. 1991. Gastropods from brackish and fresh water of the Jurassic—Cretaceous transition (a systematic reevaluation). *Berliner Geowissenschaftliche Abhandlungen Reihe A Geologie und Palaeontologie* 134:9–55.

Bandel K., Riedel F. 1994. The Late Cretaceous gastropod fauna from Ajka (Bakony Mountains, Hungary): A revision. *Annalen des Naturhistorischen Museums in Wien.* 1–65.

Barker GM. 2009. Gastropods on land: phylogeny, diversity and adaptive morphology. In: *The biology of terrestrial molluscs*. DOI: 10.1079/9780851993188.0001.

Barnosky AD., Carrasco MA. 2002. Effects of Oligo-Miocene global climate changes on mammalian species richness in the northwestern quarter of the USA. *Evolutionary Ecology Research*.

Bazin E., Glemin S., Galtier N. 2006. Population size does not influence mitochondrial genetic diversity in animals. *Science* 312:570–572. DOI: 10.1126/science.1122033.

571 Bernt M., Bleidorn C., Braband A., Dambach J., Donath A., Fritzsch G., Golombek A., Hadrys
572 H., Jühling F., Meusemann K., Middendorf M., Misof B., Perseke M., Podsiadlowski
573 L., von Reumont B., Schierwater B., Schlegel M., Schrödl M., Simon S., Stadler PF.,
574 Stöger I., Struck TH. 2013a. A comprehensive analysis of bilaterian mitochondrial
575 genomes and phylogeny. *Molecular Phylogenetics and Evolution* 69:352–364. DOI:
576 10.1016/j.ympev.2013.05.002.

577 Bernt M., Donath A., Jühling F., Externbrink F., Florentz C., Fritzsch G., Pütz J., Middendorf
578 M., Stadler PF. 2013b. MITOS: Improved de novo metazoan mitochondrial genome
579 annotation. *Molecular Phylogenetics and Evolution* 69:313–319. DOI:
580 10.1016/j.ympev.2012.08.023.

581 Bernt M., Merkle D., Ramsch K., Fritzsch G., Perseke M., Bernhard D., Schlegel M., Stadler
582 PF., Middendorf M. 2007. CREx: Inferring genomic rearrangements based on common
583 intervals. *Bioinformatics*. DOI: 10.1093/bioinformatics/btm468.

584 Böhme M. 2003. The Miocene Climatic Optimum: Evidence from ectothermic vertebrates of
585 Central Europe. *Palaeogeography, Palaeoclimatology, Palaeoecology*. DOI:
586 10.1016/S0031-0182(03)00367-5.

587 Boore JL. 1999. Animal mitochondrial genomes. *Nucleic acids research* 27:1767–80.

588 Bouchet P., Rocroi J-P., Hausdorf B., Kaim A., Kano Y., Nützel A., Parkhaev P., Schrödl M.,
589 Strong EE. 2017. Revised classification, nomenclator and typification of gastropod and
590 monoplacophoran families. *Malacologia* 61:1–526. DOI: 10.4002/040.061.0201.

591 Chen S., Zhou Y., Chen Y., Gu J. 2018. fastp: an ultra-fast all-in-one FASTQ preprocessor.
592 *Bioinformatics* 34:i884–i890. DOI: 10.1093/bioinformatics/bty560.

593 Darriba D., Taboada GL., Doallo R., Posada D. 2012. jModelTest 2: more models, new
594 heuristics and parallel computing. *Nature Methods* 9:772–772. DOI:
595 10.1038/nmeth.2109.

596 Darty K., Denise A., Ponty Y. 2009. VARNA: Interactive drawing and editing of the RNA
597 secondary structure. *Bioinformatics* 25:1974–1975. DOI:
598 10.1093/bioinformatics/btp250.

599 Dayrat B., Conrad M., Balayan S., White TR., Albrecht C., Golding R., Gomes SR.,
600 Harasewych MG., de Frias Martins AM. 2011. Phylogenetic relationships and evolution
601 of pulmonate gastropods (Mollusca): New insights from increased taxon sampling.
602 *Molecular Phylogenetics and Evolution* 59:425–437. DOI:
603 10.1016/j.ympev.2011.02.014.

604 Deng P-J., Wang W-M., Huang X-C., Wu X-P., Xie G-L., Ouyang S. 2016. The complete
605 mitochondrial genome of Chinese land snail *Mastigeulota kiangsinensis* (Gastropoda:
606 Pulmonata: Bradybaenidae). *Mitochondrial DNA* 27:1441–1442. DOI:
607 10.3109/19401736.2014.953083.

608 Dinapoli A., Klussmann-Kolb A. 2010. The long way to diversity – Phylogeny and evolution of
609 the Heterobranchia (Mollusca: Gastropoda). *Molecular Phylogenetics and Evolution*
610 55:60–76. DOI: 10.1016/j.ympev.2009.09.019.

611 Doyle J., Doyle J. 1987. A rapid isolation procedure for small amounts of leaf tissue.
612 *Phytochemical Bulletin* 19:11–15. DOI: 10.2307/4119796.

613 da Fonseca RR., Johnson WE., O'Brien SJ., Ramos MJ., Antunes A. 2008. The adaptive
614 evolution of the mammalian mitochondrial genome. *BMC Genomics* 9:119. DOI:
615 10.1186/1471-2164-9-119.

616 Friis EM., Pedersen KR., Crane PR. 2010. Diversity in obscurity: fossil flowers and the early
617 history of angiosperms. *Philosophical Transactions of the Royal Society B: Biological*
618 *Sciences* 365:369–382. DOI: 10.1098/rstb.2009.0227.

619 Gaitán-Espitia JD., Nespolo RF., Opazo JC. 2013. The Complete Mitochondrial Genome of the
620 Land Snail *Cornu aspersum* (Helicidae: Mollusca): Intra-Specific Divergence of
621 Protein-Coding Genes and Phylogenetic Considerations within Euthyneura. *PLoS ONE*
622 8. DOI: 10.1371/journal.pone.0067299.

623 Garvin MR., Bielawski JP., Gharrett AJ. 2011. Positive darwinian selection in the piston that
624 powers proton pumps in Complex I of the mitochondria of *Pacific salmon*. *PLoS ONE*
625 6. DOI: 10.1371/journal.pone.0024127.

626 Garvin MR., Bielawski JP., Sazanov LA., Gharrett AJ. 2014. Review and meta-analysis of
627 natural selection in mitochondrial complex I in metazoans. *Journal of Zoological*
628 *Systematics and Evolutionary Research* 53. DOI: 10.1111/jzs.12079.

629 González VL., Kayal E., Halloran M., Shrestha Y., Harasewych MG. 2016. The complete
630 mitochondrial genome of the land snail *Cerion incanum* (Gastropoda:
631 Stylommatophora) and the phylogenetic relationships of Cerionidae within
632 Panpulmonata. *Journal of Molluscan Studies* 82:525–533. DOI:
633 10.1093/mollus/eyw017.

634 Grande C., Templado J., Zardoya R. 2008. Evolution of gastropod mitochondrial genome
635 arrangements. *BMC Evolutionary Biology* 8:61. DOI: 10.1186/1471-2148-8-61.

636 Gray MW. 1989. Origin and evolution of mitochondrial DNA. *Annual Review of Cell Biology*.
637 DOI: 10.1146/annurev.cb.05.110189.000325.

638 Greiner S., Lehwark P., Bock R. 2019. OrganellarGenomeDRAW (OGDRAW) version 1.3.1:
639 expanded toolkit for the graphical visualization of organellar genomes. *Nucleic Acids*
640 *Research* 47:W59–W64. DOI: 10.1093/nar/gkz238.

641 Groenenberg DSJ., Harl J., Duijm E., Gittenberger E. 2017. The complete mitogenome of
642 *Orcula dolium* (Draparnaud, 1801); ultra-deep sequencing from a single long-range
643 PCR using the Ion-Torrent PGM. *Hereditas* 154:7. DOI: 10.1186/s41065-017-0028-2.

644 Groenenberg DSJ., Pirovano W., Gittenberger E., Schilthuizen M. 2012. The complete
645 mitogenome of *Cylindrus obtusus* (Helicidae, Ariantinae) using Illumina next
646 generation sequencing. *BMC Genomics* 13. DOI: 10.1186/1471-2164-13-114.

647 Hassanin A., Léger N., Deutsch J. 2005. Evidence for multiple reversals of asymmetric
648 mutational constraints during the evolution of the mitochondrial genome of Metazoa,
649 and consequences for phylogenetic inferences. *Systematic Biology* 54:277–298. DOI:
650 10.1080/10635150590947843.

651 Harasewych MG., González VL., Windsor AM., Halloran M. 2017. The complete
652 mitochondrial genome of *Cerion uva uva* (Gastropoda: Panpulmonata:
653 Stylommatophora: Cerionidae). *Mitochondrial DNA Part B* 2:159–160. DOI:
654 10.1080/23802359.2017.1303343.

655 Hatzoglou E., Rodakis GC., Lecanidou R. 1995. Complete sequence and gene organization of
656 the mitochondrial genome of the land snail *Albinaria coerulea*. *Genetics* 140:1353–
657 1366.

658 Hausdorf B. 2000. Biogeography of the Limacoidea sensu lato (Gastropoda:
659 Stylommatophora): vicariance events and long-distance dispersal. *Journal of*
660 *Biogeography* 27:379–390. DOI: 10.1046/j.1365-2699.2000.00403.x.

661 He Z-P., Dai X-B., Zhang S., Zhi T-T., Lun Z-R., Wu Z-D., Yang T-B. 2016. Complete
662 mitochondrial genome of the giant African snail, *Achatina fulica* (Mollusca:
663 Achatinidae): a novel location of putative control regions (CR) in the mitogenome
664 within Pulmonate species. *Mitochondrial DNA* 27:1084–1085. DOI:
665 10.3109/19401736.2014.930833.

666 Holznagel WE., Colgan DJ., Lydeard C. 2010. Pulmonate phylogeny based on 28S rRNA gene
667 sequences: A framework for discussing habitat transitions and character transformation.
668 *Molecular Phylogenetics and Evolution* 57:1017–1025. DOI:
669 10.1016/j.ympev.2010.09.021.

670 Hu F., Lin Y., Tang J. 2014. MLGO: phylogeny reconstruction and ancestral inference from
671 gene-order data. *BMC Bioinformatics* 15:354. DOI: 10.1186/s12859-014-0354-6.

672 Huang C-W., Lin S-M., Wu W-L. 2015. Mitochondrial genome sequences of landsnails *Aegista*
673 *diversifamilia* and *Dolicheulota formosensis* (Gastropoda: Pulmonata:
674 Stylommatophora). *Mitochondrial DNA*:1–3. DOI: 10.3109/19401736.2015.1053070.

675 Hunter SS., Settles ML., New DD., Parent CE., Gerritsen AT. 2016. Mitochondrial Genome
676 Sequence of the Galápagos Endemic Land Snail *Naesiotus nux*. *Genome*
677 *Announcements* 4. DOI: 10.1128/genomeA.01362-15.

678 Jörger KM., Stöger I., Kano Y., Fukuda H., Knebelsberger T., Schrödl M. 2010. On the origin
679 of Acochlidia and other enigmatic euthyneuran gastropods, with implications for the
680 systematics of Heterobranchia. *BMC Evolutionary Biology*. DOI: 10.1186/1471-2148-
681 10-323.

682 Kano Y., Brenzinger B., Nützel A., Wilson NG., Schrödl M. 2016. Ringiculid bubble snails
683 recovered as the sister group to sea slugs (Nudipleura). *Scientific Reports* 6:30908. DOI:
684 10.1038/srep30908.

685 Katoh K., Standley DM. 2013. MAFFT Multiple Sequence Alignment Software Version 7:
686 Improvements in Performance and Usability. *Molecular Biology and Evolution* 30:772–
687 780. DOI: 10.1093/molbev/mst010.

688 Kearse M., Moir R., Wilson A., Stones-Havas S., Cheung M., Sturrock S., Buxton S., Cooper
689 A., Markowitz S., Duran C., Thierer T., Ashton B., Meintjes P., Drummond A. 2012.
690 Geneious Basic: an integrated and extendable desktop software platform for the
691 organization and analysis of sequence data. *Bioinformatics* (Oxford, England) 28:1647–
692 9. DOI: 10.1093/bioinformatics/bts199.

693 Korábek O., Petrusek A., Rovatsos M. 2019. The complete mitogenome of Helix pomatia and
694 the basal phylogeny of Helicinae (Gastropoda, Stylommatophora, Helicidae). *ZooKeys*
695 827:19–30. DOI: 10.3897/zookeys.827.33057.

696 Kumar S., Stecher G., Tamura K. 2016. MEGA7: Molecular Evolutionary Genetics Analysis
697 Version 7.0 for Bigger Datasets. *Molecular Biology and Evolution* 33:1870–4. DOI:
698 10.1093/molbev/msw054.

699 Lanfear R., Calcott B., Ho SYW., Guindon S. 2012. PartitionFinder: Combined selection of
700 partitioning schemes and substitution models for phylogenetic analyses. *Molecular*
701 *Biology and Evolution* 29:1695–1701. DOI: 10.1093/molbev/mss020.

702 Laslett D., Canbäck B. 2008. ARWEN: A program to detect tRNA genes in metazoan
703 mitochondrial nucleotide sequences. *Bioinformatics* 24:172–175. DOI:
704 10.1093/bioinformatics/btm573.

705 Li X-D., Jiang G-F., Yan L-Y., Li R., Mu Y., Deng W-A. 2018. Positive Selection Drove the
706 Adaptation of Mitochondrial Genes to the Demands of Flight and High-Altitude
707 Environments in Grasshoppers. *Frontiers in Genetics* 9. DOI:
708 10.3389/fgene.2018.00605.

709 Lin J-H., Zhou W., Ding H-L., Wang P., Ai H-M. 2016. The mitochondrial genome of the land
710 snail *Cernuella virgata* (Da Costa, 1778): the first complete sequence in the family
711 Hygromiidae (Pulmonata, Stylommatophora). *ZooKeys* 589:55–69. DOI:
712 10.3897/zookeys.589.7637.

713 Liu G-H., Wang S-Y., Huang W-Y., Zhao G-H., Wei S-J., Song H-Q., Xu M-J., Lin R-Q.,
714 Zhou D-H., Zhu X-Q. 2012. The Complete Mitochondrial Genome of *Galba pervia*
715 (Gastropoda: Mollusca), an Intermediate Host Snail of *Fasciola* spp. *PLoS ONE*
716 7:e42172. DOI: 10.1371/journal.pone.0042172.

717 Meiklejohn CD., Montooth KL., Rand DM. 2007. Positive and negative selection on the
718 mitochondrial genome. *Trends in Genetics*: TIG 23:259–63. DOI:
719 10.1016/j.tig.2007.03.008.

720 Melo-Ferreira J., Vilela J., Fonseca MM., Da Fonseca RR., Boursot P., Alves PC. 2014. The
721 elusive nature of adaptive mitochondrial DNA evolution of an arctic lineage prone to
722 frequent introgression. *Genome Biology and Evolution* 6:886–896. DOI:
723 10.1093/gbe/evu059.

724 Meng G., Li Y., Yang C., Liu S. 2019. MitoZ: a toolkit for animal mitochondrial genome
725 assembly, annotation and visualization. *Nucleic Acids Research*. DOI:
726 10.1093/nar/gkz173.

727 Minton RL., Martinez Cruz MA., Farman ML., Perez KE. 2016. Two complete mitochondrial
728 genomes from *Praticolella mexicana* Perez, 2011 (Polygyridae) and gene order
729 evolution in Helicoidea (Mollusca, Gastropoda). *ZooKeys* 626:137–154. DOI:
730 10.3897/zookeys.626.9633.

731 Morales HE., Pavlova A., Joseph L., Sunnucks P. 2015. Positive and purifying selection in
732 mitochondrial genomes of a bird with mitonuclear discordance. *Molecular Ecology*
733 24:2820–2837. DOI: 10.1111/mec.13203.

734 Moritz C., Dowling TE., Brown WM. 1987. Evolution of Animal Mitochondrial DNA:
735 Relevance for Population Biology and Systematics. *Annual Review of Ecology and*
736 *Systematics* 18:269–292. DOI: 10.1146/annurev.es.18.110187.001413.

737 Murrell B., Moola S., Mabona A., Weighill T., Sheward D., Kosakovsky Pond SL., Scheffler
738 K. 2013. FUBAR: A fast, unconstrained Bayesian approximation for inferring selection.
739 *Molecular Biology and Evolutio*n 30:1196–1205. DOI: 10.1093/molbev/mst030.

740 Murrell B., Wertheim JO., Moola S., Weighill T., Scheffler K., Kosakovsky Pond SL. 2012.
741 Detecting individual sites subject to episodic diversifying selection. *PLoS Genetics*
742 8:e1002764. DOI: 10.1371/journal.pgen.1002764.

743 Ojala D., Montoya J., Attardi G. 1981. tRNA punctuation model of RNA processing in human
744 mitochondria. *Nature* 290:470–474. DOI: 10.1038/290470a0.

745 Osca D., Templado J., Zardoya R. 2014. The mitochondrial genome of *Ifremeria nautilei* and
746 the phylogenetic position of the enigmatic deep-sea Abyssochrysoidea (Mollusca:
747 Gastropoda). *Gene* 547:257–266. DOI: 10.1016/j.gene.2014.06.040.

748 Perna NT., Kocher TD. 1995. Patterns of nucleotide composition at fourfold degenerate sites of
749 animal mitochondrial genomes. *Journal of Molecular Evolution* 41:353–358. DOI:
750 10.1007/BF01215182.

751 Ponder WF., Lindberg DR. 1997. Towards a phylogeny of gastropod molluscs: an analysis
752 using morphological characters. *Zoological Journal of the Linnean Society* 119:83–265.
753 DOI: 10.1006/zjls.1996.0066.

754 Price MR., Forsman ZH., Knapp I., Hadfield MG., Toonen RJ. 2016a. The complete
755 mitochondrial genome of *Achatinella mustelina* (Gastropoda: Pulmonata:
756 Stylommatophora). *Mitochondrial DNA Part B* 1:175–177. DOI:
757 10.1080/23802359.2016.1149787.

758 Price MR., Forsman ZH., Knapp IS., Toonen RJ., Hadfield MG. 2016b. The complete
759 mitochondrial genome of *Achatinella sowerbyana* (Gastropoda: Pulmonata:
760 Stylommatophora: Achatinellidae). *Mitochondrial DNA Part B* 1:666–668. DOI:
761 10.1080/23802359.2016.1219631.

762 Price MR., Forsman ZH., Knapp I., Toonen RJ., Hadfield MG. 2018. A comparison of
763 mitochondrial genomes from five species in three genera suggests polyphyly in the
764 subfamily Achatinellinae (Gastropoda: Pulmonata: Stylommatophora: Achatinellidae).
765 *Mitochondrial DNA Part B* 3:611–612. DOI: 10.1080/23802359.2018.1473737.

766 Rambaut A. 2012. FigTree v1. 4.0. A graphical viewer of phylogenetic trees. Institute of
767 Evolutionary Biology University of Edinburgh.

768 Rambaut A., Drummond AJ., Xie D., Baele G., Suchard MA. 2018. Posterior Summarization in
769 Bayesian Phylogenetics Using Tracer 1.7. *Systematic Biology* 67:901–904. DOI:
770 10.1093/sysbio/syy032.

771 Rand DM. 2001. The units of selection on mitochondrial DNA. *Annual Review of Ecology and*
772 *Systematics* 32:415–448. DOI: 10.1146/annurev.ecolsys.32.081501.114109.

773 Razkin O., Gómez-Moliner BJ., Prieto CE., Martínez-Ortí A., Arrébola JR., Muñoz B., Chueca
774 LJ., Madeira MJ. 2015. Molecular phylogeny of the western Palaearctic Helicoidea
775 (Gastropoda, Stylommatophora). *Molecular Phylogenetics and Evolution*. DOI:
776 10.1016/j.ympev.2014.11.014.

777 Reyes A., Gissi C., Pesole G., Saccone C. 1998. Asymmetrical directional mutation pressure in
778 the mitochondrial genome of mammals. *Molecular Biology and Evolution*. DOI:
779 10.1093/oxfordjournals.molbev.a026011.

780 Rice P., Longden L., Bleasby A. 2000. EMBOSS: The European Molecular Biology Open
781 Software Suite. *Trends in Genetics*. DOI: 10.1016/S0168-9525(00)02024-2.

782 De Rijk P., Wuyts J., De Wachter R. 2003. RnaViz 2: an improved representation of RNA
783 secondary structure. *Bioinformatics* (Oxford, England) 19:299–300.

784 Romero PE., Weigand AM., Pfenninger M. 2016. Positive selection on panpulmonate
785 mitogenomes provide new clues on adaptations to terrestrial life. *BMC Evolutionary*
786 *Biology* 16:164. DOI: 10.1186/s12862-016-0735-8.

787 Ronquist F., Teslenko M., van der Mark P., Ayres DL., Darling A., Höhna S., Larget B., Liu
788 L., Suchard MA., Huelsenbeck JP. 2012. MrBayes 3.2: Efficient Bayesian Phylogenetic
789 Inference and Model Choice Across a Large Model Space. *Systematic Biology* 61:539–
790 542. DOI: 10.1093/sysbio/sys029.

791 Roth B., Poinar GO., Acra A., Acra F. 1996. Probable Pupillid land snail of Early Cretaceous
792 (Hauterivian) age in amber from Lebanon. *Veliger* 39:87–88.

793 Sevigny JL., Kirouac LE., Thomas WK., Ramsdell JS., Lawlor KE., Sharifi O., Grewal S.,
794 Baysdorfer C., Curr K., Naimie AA., Okamoto K., Murray JA., Newcomb JM. 2015.
795 The mitochondrial genomes of the Nudibranch mollusks, *Melibe leonina* and *Tritonia*
796 *diomedea*, and their impact on gastropod phylogeny. *PLoS ONE* 10:e0127519. DOI:
797 10.1371/journal.pone.0127519.

798 Sharma L., Lu J., Bai Y. 2009. Mitochondrial Respiratory Complex I: Structure, Function and
799 Implication in Human Diseases. *Current Medicinal Chemistry*. DOI:
800 10.2174/092986709787846578.

801 Smith MD., Wertheim JO., Weaver S., Murrell B., Scheffler K., Kosakovsky Pond SL. 2015.
802 Less is more: An adaptive branch-site random effects model for efficient detection of
803 episodic diversifying selection. *Molecular Biology and Evolution* 32:1342–1353. DOI:
804 10.1093/molbev/msv022.

805 Solem A., Yochelson EL. 1979. North American Paleozoic land snails, with a summary of
806 other Paleozoic non-marine snails. *Geological Survey Professional Paper*.

807 Song L., Florea L., Langmead B. 2014. Lighter: fast and memory-efficient sequencing error
808 correction without counting. *Genome Biology* 15:509. DOI: 10.1186/s13059-014-0509-
809 9.

810 Stamatakis A. 2014. RAxML version 8: a tool for phylogenetic analysis and post-analysis of
811 large phylogenies. *Bioinformatics* 30:1312–1313. DOI: 10.1093/bioinformatics/btu033.

812 Stöger I., Schrödl M. 2013. Mitogenomics does not resolve deep molluscan relationships
813 (yet?). *Molecular Phylogenetics and Evolution* 69:376–392. DOI:
814 10.1016/j.ympev.2012.11.017.

815 Sun BN., Wei LL., Shen HD., Wu HX., Wang DF. 2016. Phylogenetic analysis of euthyneuran
816 gastropods from sea to land mainly based on comparative mitogenomic of four species
817 of Onchidiidae (Mollusca: Gastropoda: Pulmonata). *Mitochondrial DNA Part A*
818 27:3075–3077. DOI: 10.3109/19401736.2014.1003916.

819 Swofford DL. 2002. Phylogenetic Analysis Using Parsimony (*and Other Methods). Version 4.
820 Sunderland, Massachusetts, USA: Sinauer Associates.

821 Tillier S., Masselmot M., Tillirt A. 1996. Phylogenetic relationships of the Pulmonate
822 Gastropods from rRNA sequences, and tempo and age of the Stylommatophoran

radiation. In: Taylor JD ed. Origin and Evolutionary Radiation of the Mollusca. *Oxford: Oxford Press*, 267–284.

Tolley KA., Chase BM., Forest F. 2008. Speciation and radiations track climate transitions since the Miocene Climatic Optimum: a case study of southern African chameleons. *Journal of Biogeography* 35:1402–1414. DOI: 10.1111/j.1365-2699.2008.01889.x.

Uribe JE., Colgan D., Castro LR., Kano Y., Zardoya R. 2016a. Phylogenetic relationships among superfamilies of Neritimorpha (Mollusca: Gastropoda). *Molecular Phylogenetics and Evolution* 104:21–31. DOI: 10.1016/j.ympev.2016.07.021.

Uribe JE., Kano Y., Templado J., Zardoya R. 2016b. Mitogenomics of Vetigastropoda: insights into the evolution of pallial symmetry. *Zoologica Scripta* 45:145–159. DOI: 10.1111/zsc.12146.

Uribe JE., Williams ST., Templado J., Abalde S., Zardoya R. 2017. Denser mitogenomic sampling improves resolution of the phylogeny of the superfamily Trochoidea (Gastropoda: Vetigastropoda). *Journal of Molluscan Studies* 83:111–118. DOI: 10.1093/mollus/eyw049.

Vaidya G., Lohman DJ., Meier R. 2011. SequenceMatrix: concatenation software for the fast assembly of multi-gene datasets with character set and codon information. *Cladistics* 27:171–180. DOI: 10.1111/j.1096-0031.2010.00329.x.

Vicentini A., Barber JC., Aliscioni SS., Giussani LM., Kellogg EA. 2008. The age of the grasses and clusters of origins of C4 photosynthesis. *Global Change Biology*. DOI: 10.1111/j.1365-2486.2008.01688.x.

844 Wade CM., Mordan PB., Clarke B. 2001. A phylogeny of the land snails (Gastropoda:
845 Pulmonata). *Proceedings of the Royal Society of London. Series B: Biological Sciences*
846 268:413–422. DOI: 10.1098/rspb.2000.1372.

847 Wade CM., Mordan PB., Naggs F. 2006. Evolutionary relationships among the Pulmonate land
848 snails and slugs (Pulmonata, Stylommatophora). *Biological Journal of the Linnean*
849 *Society*. DOI: 10.1111/j.1095-8312.2006.00596.x.

850 Wang P., Yang H., Zhou W., Hwang C., Zhang W., Qian Z. 2014. The mitochondrial genome
851 of the land snail *Camaena cicatricosa* (Müller, 1774) (Stylommatophora, Camaenidae):
852 the first complete sequence in the family Camaenidae. *ZooKeys* 451:33–48. DOI:
853 10.3897/zookeys.451.8537.

854 Weaver S., Shank SD., Spielman SJ., Li M., Muse S V., Kosakovsky Pond SL. 2018.
855 Datamonkey 2.0: A modern web application for characterizing selective and other
856 evolutionary processes. *Molecular Biology and Evolution* 35:773–777. DOI:
857 10.1093/molbev/msx335.

858 White TR., Conrad MM., Tseng R., Balayan S., Golding R., de Frias Martins AM., Dayrat BA.
859 2011. Ten new complete mitochondrial genomes of pulmonates (Mollusca: Gastropoda)
860 and their impact on phylogenetic relationships. *BMC Evolutionary Biology* 11:295.
861 DOI: 10.1186/1471-2148-11-295.

862 Williams ST., Foster PG., Littlewood DTJ. 2014. The complete mitochondrial genome of a
863 turbinid vetigastropod from MiSeq Illumina sequencing of genomic DNA and steps
864 towards a resolved gastropod phylogeny. *Gene* 533:38–47. DOI:
865 10.1016/j.gene.2013.10.005.

Wolstenholme DR. 1992. Animal Mitochondrial DNA: Structure and Evolution. *International Review of Cytology* 141:173–216. DOI: 10.1016/S0074-7696(08)62066-5.

Woolley S., Johnson J., Smith MJ., Crandall KA., McClellan DA. 2003. TreeSAAP: Selection on amino acid properties using phylogenetic trees. *Bioinformatics* 19:671–672. DOI: 10.1093/bioinformatics/btg043.

Xie J., Feng J., Guo Y., Ye Y., Li J., Guo B. 2019a. The complete mitochondrial genome and phylogenetic analysis of *Nerita yoldii* (Gastropoda: Neritidae). *Mitochondrial DNA Part B* 4:1099–1100. DOI: 10.1080/23802359.2019.1586485.

Xie G-L., Köhler F., Huang X-C., Wu R-W., Zhou C-H., Ouyang S., Wu X-P. 2019b. A novel gene arrangement among the Stylommatophora by the complete mitochondrial genome of the terrestrial slug *Meghimatium bilineatum* (Gastropoda, Arionoidea). Molecular Phylogenetics and Evolution 135:177–184. DOI: 10.1016/j.ympev.2019.03.002.

Yamazaki N., Ueshima R., Terrett JA., Yokobori SI., Kaifu M., Segawa R., Kobayashi T., Numachi KI., Ueda T., Nishikawa K., Watanabe K., Thomas RH. 1997. Evolution of pulmonate gastropod mitochondrial genomes: Comparisons of gene organizations of *Euhadra*, *Cepaea* and *Albinaria* and implications of unusual tRNA secondary structures. *Genetics* 145:749–758.

Yang Z. 2007. PAML 4: Phylogenetic Analysis by Maximum Likelihood. *Molecular Biology and Evolution* 24:1586–1591. DOI: 10.1093/molbev/msm088.

Yang X., Xie G-L., Wu X-P., Ouyang S. 2016. The complete mitochondrial genome of Chinese land snail *Aegista aubryana* (Gastropoda: Pulmonata: Bradybaenidae). *Mitochondrial DNA Part A* 27:3538–3539. DOI: 10.3109/19401736.2015.1074207.

888 Yang T., Xu G., Gu B., Shi Y., Mzuka HL., Shen H. 2019. The Complete Mitochondrial
889 Genome Sequences of the *Philomycus bilineatus* (Stylommatophora: Philomycidae) and
890 Phylogenetic Analysis. *Genes* 10:198. DOI: 10.3390/genes10030198.

891 Zapata F., Wilson NG., Howison M., Andrade SCS., Jörger KM., Schrödl M., Goetz FE.,
892 Giribet G., Dunn CW. 2014. Phylogenomic analyses of deep gastropod relationships
893 reject Orthogastropoda. *Proceedings of the Royal Society B: Biological Sciences*
894 281:20141739. DOI: 10.1098/rspb.2014.1739.

895 Zuker M. 2003. Mfold web server for nucleic acid folding and hybridization prediction. *Nucleic*
896 *Acids Research*.

897

898

899 **Figure Legends**

900 **Figure 1. Mitogenome organization of *Arion vulgaris*.** Genes transcribed from the J and N
901 strands are shown outside and inside of the circle, respectively. PCGs coding complex I,
902 complex III, complex IV and complex V components are marked with yellow, purple, pink and
903 green, respectively. rRNA genes are coloured with red and putative control region is coloured
904 with cyan, while tRNA genes are coloured with dark blue and labelled by the single letter
905 amino acid code.

906 **Figure 2. Relative synonymous codon usage (RSCU) of the *A. vulgaris* and *A. rufus***
907 **mitogenomes.** Codon families are provided on the x axis. The stop codons are not given.

908 **Figure 3**. **Predicted secondary structure of putative control region of *A. vulgaris***
909 **mitogenome.** Nucleotides are coloured as follows: Adenine is green, thymine is red, cytosine is
910 blue and guanine is black. The poly-T stretch is labelled with purple.

911 **Figure 4. Stylommatophoran phylogenetic tree constructed under BI using the dataset**
912 **8P12RNA.** *Carychium tridentatum* (Ellobioidea), *Platevindex mortoni* (Systellommatophora)
913 and *Galba pervia* (Hygrophila) are used as outgroup. Only support values <0.95 (posterior
914 probabilities) are shown. Nodes are labelled with numbers refers to hypothetical ancestral
915 mitogenome organizations inferred by MLGO.

916 **Figure 5. Dated phylogenetic tree.** The axis on the bottom refers to Ma. Letters in the boxes
917 refers to external calibration points.

918

919

920

921

922 **Supplementary Figure Legends**

923 **Figure S1.** Predicted secondary structures for the 22 typical tRNA genes of *A. vulgaris*
924 mitogenome. Watson–Crick pairs are indicated by lines and wobble GU pairs are indicated by
925 dots.

926 **Figure S2.** The phylogenetic tree constructed under ML using the dataset 8P12RNA. Only
927 support values <100% (bootstraps) are shown.

928 **Figure S3.** The phylogenetic tree constructed under BI using the dataset P123RNA. Only
929 support values <1.00 (posterior probabilities) are shown.

930 **Figure S4.** Stylommatophoran phylogenetic tree constructed under ML using the dataset
931 P123RNA. Only support values <100% (bootstraps) are shown.

Figure 1

Mitogenome organization of *Arion vulgaris*.

Genes transcribed from the J and N strands are shown outside and inside of the circle, respectively. PCGs coding complex I, complex III, complex IV and complex V components are marked with yellow, purple, pink and green, respectively. rRNA genes are coloured with red and putative control region is coloured with cyan, while tRNA genes are coloured with dark blue and labelled by the single letter amino acid code.

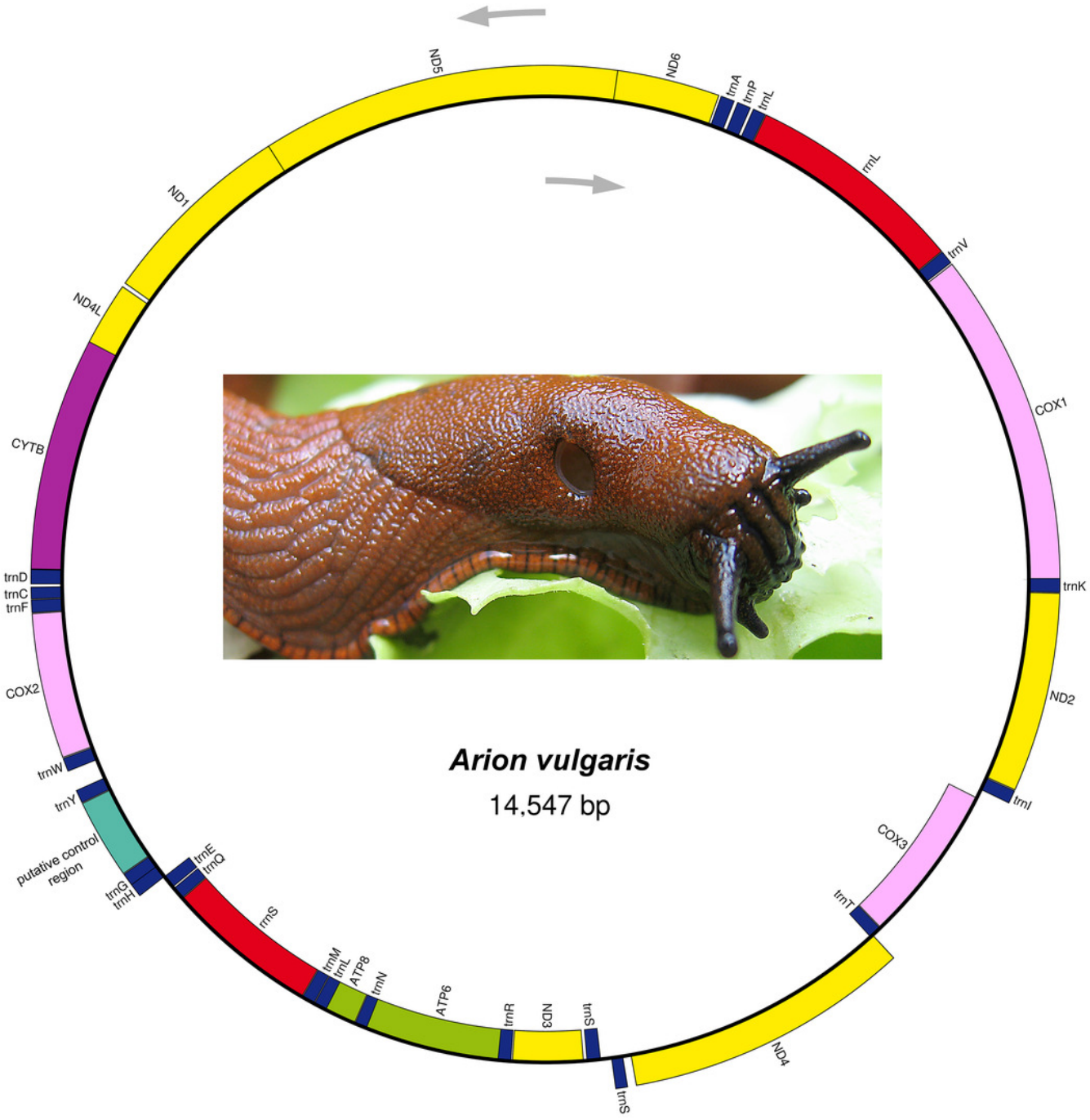
ND5
ND6
trnA
trnP
trnL
rrnL
trnV
COX1
trnK
ND2
trnI
COX3
trnT
ND4
trnS
ND3
trnR
ATP6
trnN
ATP8
trnL
rrnS
trnM
trnE
trnQ
trnG
trnH
putative control region
trnY
trnW
COX2
trnD
trnC
trnF
CYTB
ND4L
ND1
Arion vulgaris
14,547 bp

Figure 2

Relative synonymous codon usage (RSCU) of the *A. vulgaris* and *A. rufus* mitogenomes.

Codon families are provided on the x axis. The stop codons are not given.

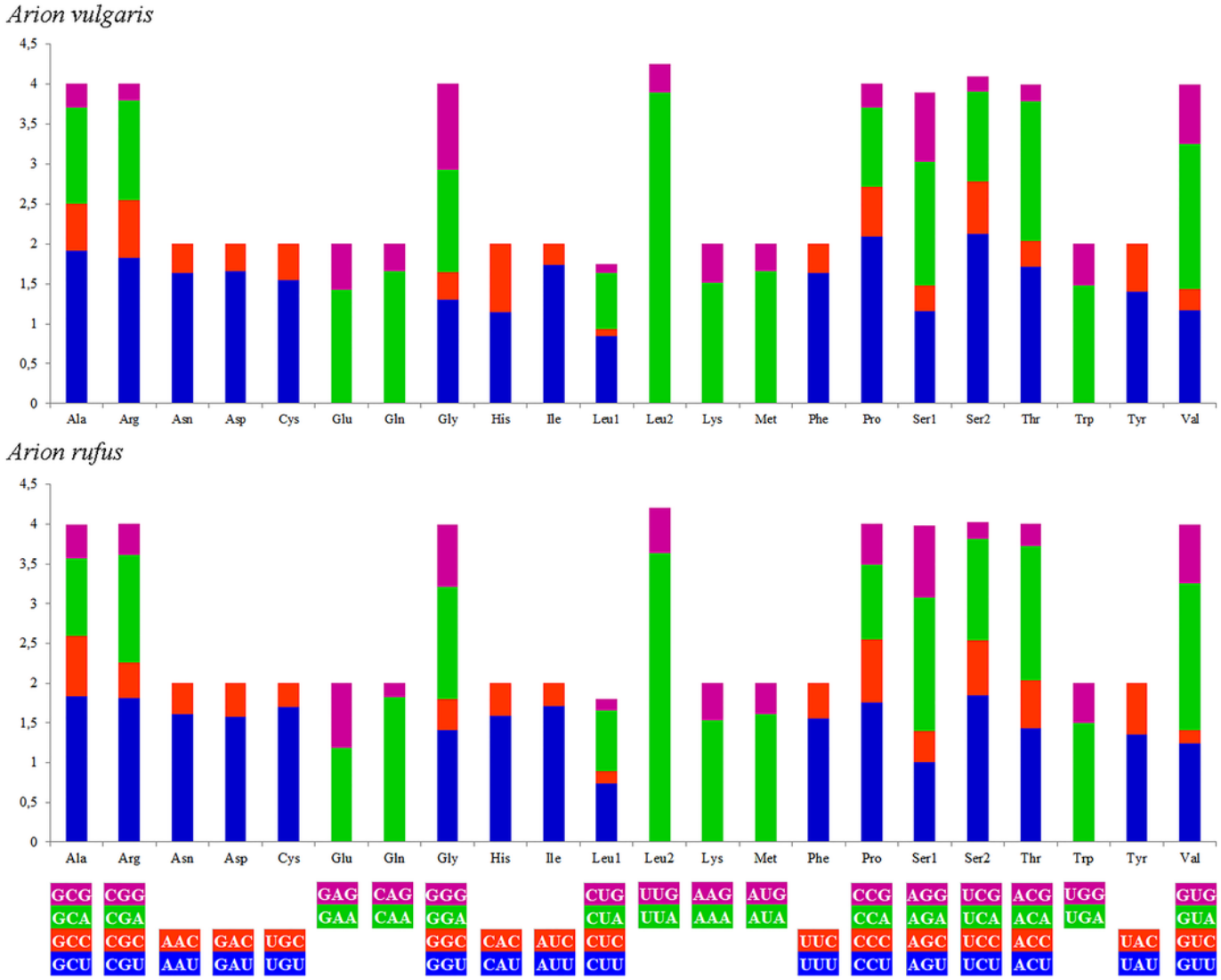

Figure 3

Predicted secondary structure of putative control region of *A. vulgaris* mitogenome.

Nucleotides are coloured as follows: Adenine is green, thymine is red, cytosine is blue and guanine is black. The poly-T stretch is labelled with purple.

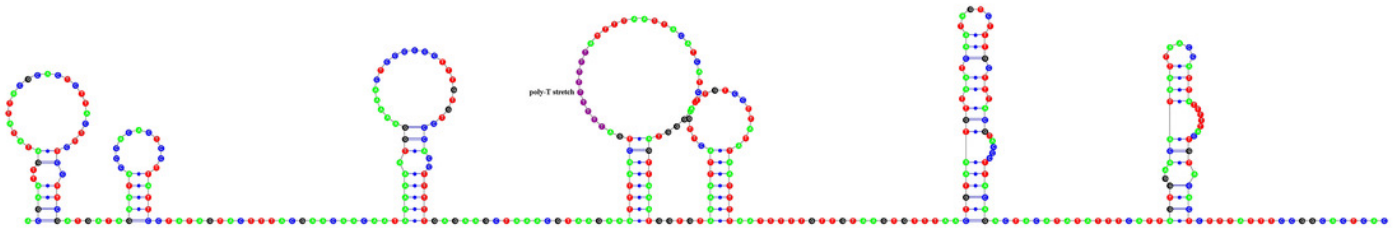

Figure 4

Stylommatophoran phylogenetic tree constructed under BI using the dataset 8P12RNA.

Carychium tridentatum (Ellobioidea), *Platevindex mortoni* (Systellommatophora) and *Galba pervia* (Hygrophila) are used as outgroup. Only support values <0.95 (posterior probabilities) are shown. Nodes are labelled with numbers refers to hypothetical ancestral mitogenome organizations inferred by MLGO.

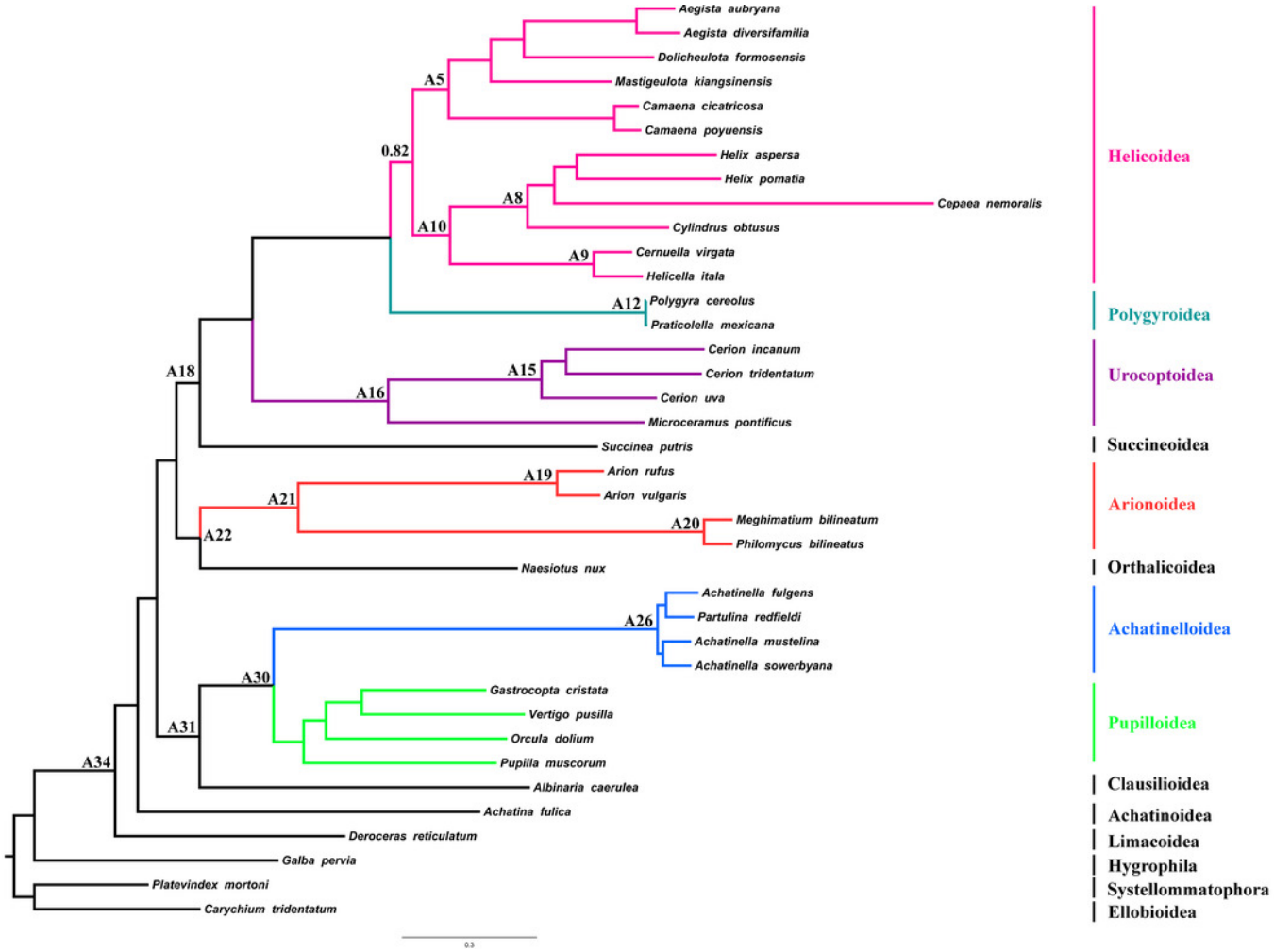

Figure 5

Dated phylogenetic tree.

The axis on the bottom refers to Ma. Letters in the boxes refers to external calibration points.

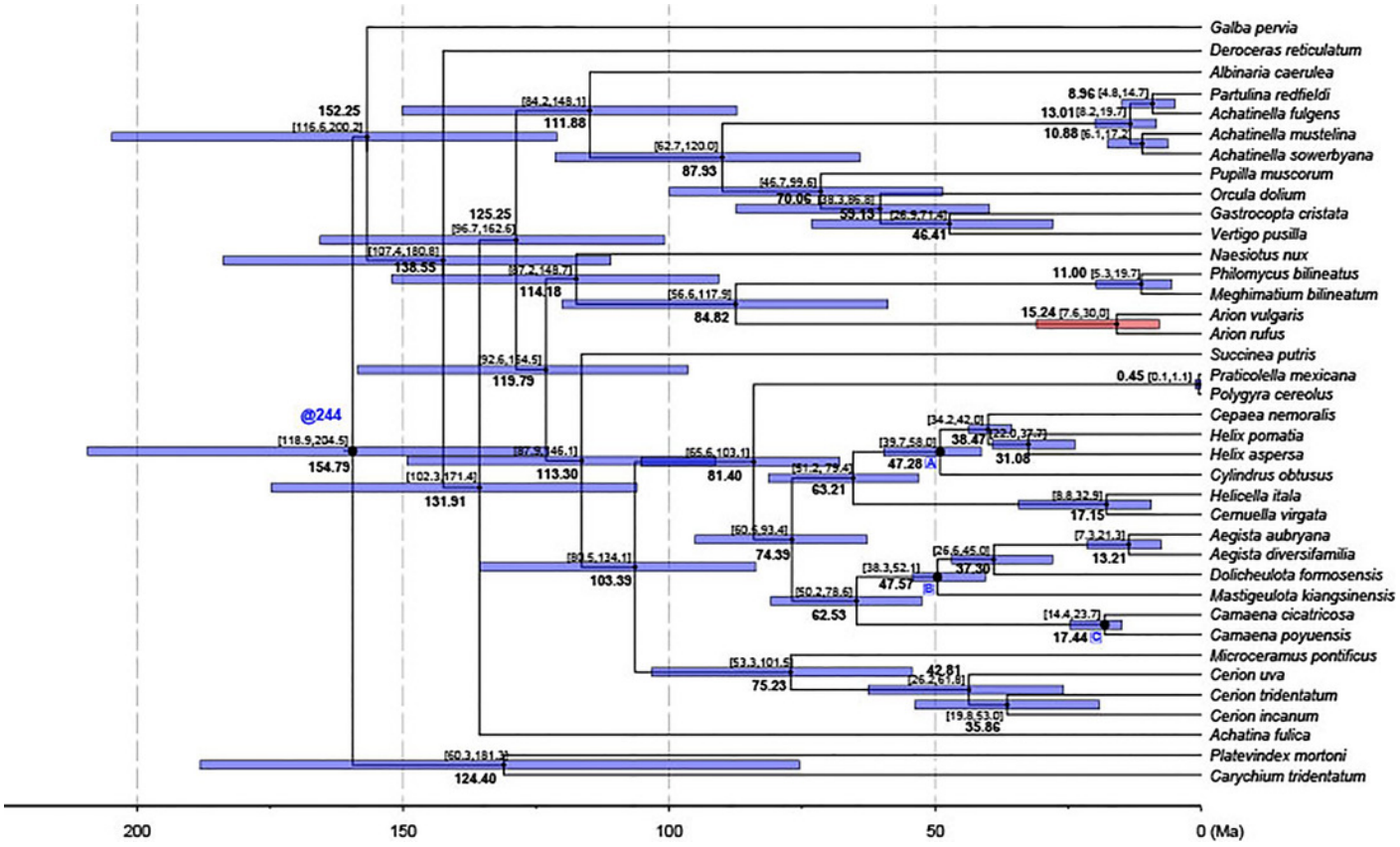

Table 1(on next page)

List of stylommatophoran mitogenomes used in phylogenetic and comparative analyses

Table 1. List of stylommatophoran mitogenomes used in phylogenetic and comparative analyses

	Species	Family	Accession number	References
	Arion vulgaris	Arionidae	Pending	This study
	Achatinella fulgens	Achatinellidae	MG925058	Price et al., (2018)
	Achatinella mustelina	Achatinellidae	NC030190	Price et al., (2016a)
	Achatinella sowerbyana	Achatinellidae	KX356680	Price et al., (2016b)
	Partulina redfieldi	Achatinellidae	MG925057	Price et al., (2018)
	Achatina fulica	Achatinidae	KM114610	He et al., (2016)
	Arion rufus	Arionidae	KT626607	Romero et al. (2016)
	Meghimatium bilineatum	Philomycidae	NC035429	Xie et al., (2019)
	Philomycus bilineatus	Philomycidae	MG722906	Yang et al., (2019)
	Camaena cicatricosa	Camaenidae	NC025511	Wang et al., (2014)
	Camaena poyuensis	Camaenidae	KT001074	Unpublished
	Albinaria caerulea	Clausiliidae	NC001761	Hatzoglou et al., (1995)
	Aegista aubryana	Bradybaenidae	NC029419	Yang et al., (2016)
	Aegista diversifamilia	Bradybaenidae	NC027584	Huang, Lin & Wu, (2015)
	Dolicheulota formosensis	Bradybaenidae	NC027493	Huang, Lin & Wu, (2015)
	Mastigeulota kiangsinensis	Bradybaenidae	NC024935	Deng et al., (2016)
	Cernuella virgata	Geomitridae	NC030723	Lin et al., (2016)
	Helicella itala	Geomitridae	KT696546	Romero et al. (2016)
	Cepaea nemoralis	Helicidae	NC001816	Yamazaki et al., (1997)
	Cylindrus obtusus	Helicidae	NC017872	Groenenberg et al., (2012)
	Helix aspersa	Helicidae	NC021747	Gaitán-Espitia et al., (2013)
	Helix pomatia	Helicidae	NC041247	Korábek et al., (2019)
	Deroceras reticulatum	Agriolimacidae	NC035495	Ahn et al., (2017)
	Naesiotus nux	Orthalicidae	NC028553	Hunter et al., (2016)
	Polygyra cereolus	Polygyridae	NC032036	Unpublished
	Praticolella mexicana	Polygyridae	KX240084	Minton et al., (2016)
	Orcula dolium	Orculidae	NC034782	Groenenberg et al., (2017)
	Gastrocopta cristata	Gastrocoptidae	NC026043	Unpublished
	Pupilla muscorum	Pupillidae	NC026044	Unpublished
	Vertigo pusilla	Vertiginidae	NC026045	Unpublished
	Succinea putris	Succineidae	NC016190	White et al., (2011)
	Cerion incanum	Cerionidae	NC025645	González et al., (2016)
	Cerion tridentatum costellata	Cerionidae	KY249249	Unpublished
	Cerion uva	Cerionidae	KY124261	Harasewych et al., (2017)
	Microceramus pontificus	Urocoptidae	NC036381	Unpublished
Ellobioidea	*Carychium tridentatum*	Ellobiidae	KT696545	Romero et al. (2016)
Hygrophila	*Galba pervia*	Lymnaeidae	NC018536	Liu et al., (2012)
Systellommatophora	*Platevindex mortoni*	Onchidiidae	GU475132	Sun et al., (2016)

Table 2(on next page)

Mitogenome summary of *Arion vulgaris*

Table 2. Mitogenome summary of *Arion vulgaris*

Gene	Strand	From	To	Size	Start codon	Stop codon	Anticodon	IGN
COX1	J	1	1530	1530	TTG	TAG		4
tRNA-Val	J	1535	1600	66			UAC	0
16S rRNA	J	1601	2613	1013				0
tRNA-Leu	J	2614	2675	62			UAG	11
tRNA-Pro	J	2687	2752	66			UGG	13
tRNA-Ala	J	2766	2831	66			UGC	7
ND6	J	2839	3312	474	ATG	TAG		-41
ND5	J	3272	4960	1689	ACA	TAA		-10
ND1	J	4951	5853	903	ATG	TAG		15
ND4L	J	5869	6163	295	ATA	T-		-15
CYTB	J	6149	7228	1080	ATG	TAA		-2
tRNA-Asp	J	7227	7296	70			GUC	10
tRNA-Cys	J	7307	7363	57			GCA	0
tRNA-Phe	J	7364	7425	62			GAA	0
COX2	J	7426	8094	669	ATG	TAG		1
tRNA-Trp	J	8096	8160	65			UCA	91
tRNA-Tyr	J	8252	8315	67			GUA	0
Control region	J	8316	8685	370				0
tRNA-Gly	J	8686	8763	78			UCC	-20
tRNA-His	J	8744	8809	66			GUG	-3
tRNA-Glu	N	8807	8873	67			UUC	5
tRNA-Gln	N	8879	8942	64			UUG	0
12S rRNA	N	8943	9689	747				0
tRNA-Met	N	9690	9754	65			CAU	0
tRNA-Leu	N	9755	9820	66			UAA	-32
ATP8	N	9789	9971	183	GTG	TAA		0
tRNA-Asn	N	9972	10033	62			GUU	-8
ATP6	N	10026	10688	663	ATA	TAA		-9
tRNA-Arg	N	10680	10746	67			UCG	3
ND3	N	10750	11094	345	ATG	TAA		13
tRNA-Ser2	N	11108	11176	69			UGA	49
tRNA-Ser1	J	11226	11283	58			GCU	36
ND4	J	11320	12633	1314	ATA	TAG		-18
tRNA-Thr	N	12616	12681	66			UGU	0
COX3	N	12682	13462	781	ATG	T-		41
tRNA-Ile	J	13504	13567	64			GAU	1
ND2	J	13569	14486	918	ATG	TAA		0
tRNA-Lys	J	14487	6	67			UUU	-6

J. major; N. minor; IGN, intergenic nucleotides. Minus indicates overlapping sequences between adjacent genes.

4

Table 3(on next page)

Nucleotide composition of the *Arion vulgaris* mitogenome

Table 3. Nucleotide composition of the *Arion vulgaris* mitogenome

Feature	T%	C%	A%	G%	A+T%	AT-skew	GC-skew
Whole genome	37.75	14.26	32.45	15.54	70.20	-0.076	0.043
Protein coding genes	39.90	14.61	29.44	16.05	69.34	-0.151	0.047
First codon position	33.54	14.01	30.64	21.81	64.18	-0.045	0.218
Second codon position	45.65	19.42	18.55	16.38	64.21	-0.422	-0.085
Third codon position	40.50	10.39	39.14	9.97	79.64	-0.017	-0.021
Protein coding genes-J	39.78	14.34	29.72	16.16	69.50	-0.145	0.060
First codon position-J	32.94	13.93	31.23	21.90	64.17	-0.027	0.222
Second codon position-J	45.91	19.07	18.53	16.49	64.44	-0.425	-0.073
Third codon position-J	40.50	10.01	39.41	10.08	79.90	-0.014	0.003
Protein coding genes-N	40.42	15.80	28.19	15.60	68.60	-0.178	-0.006
First codon position-N	36.24	14.37	27.98	21.41	64.22	-0.129	0.197
Second codon position-N	44.50	20.95	18.65	15.90	63.15	-0.409	-0.137
Third codon position-N	40.52	12.08	37.92	9.48	78.44	-0.033	-0.121
tRNA genes	36.40	11.48	36.33	15.80	72.72	-0.001	0.158
rRNA genes	33.24	13.58	38.18	15.00	71.42	0.069	0.050
Control region	38.92	18.65	30.81	11.62	69.73	-0.116	-0.232

Table 4(on next page)

Likelihood ratios of PAML analysis showing different selective pressures on the mitochondrial PCGs in Stylommatophora

Table 4. Likelihood ratios of PAML analysis showing different selective pressures on the mitochondrial PCGs in Stylommatophora

Models[a]		A		B		C		A-B		B-C	
Gene	ω	lnL[b]	Np[c]	lnL	Np	lnL	Np	LRT	P	LRT	P[d]
ATP6	0,0509	-19658.6890		-19377.7446		-19374.7961		561.8887	0.000	-5.896982	**0.015**
ATP8	0,2198	-6460.1406		-6355.5745		-6355.5745		209.1322	0.000	-0.000006	1.000
COX1	0,0129	-26428.6827		-26169.9332		-26169.9332		517.4990	0.000	0.000000	1.000
COX2	0,0393	-16022.1910		-15851.6973		-15848.6152		340.9874	0.000	-6.164250	**0.013**
COX3	0,0317	-18617.4781		-18345.8456		-18341.7284		543.2650	0.000	-8.234404	**0.004**
CYTB	0,0416	-26893.7004		-26297.6496		-26297.6496		1192.1017	0.000	0.000082	0.992
ND1	0,0430	-24857.6972	76	-24528.7292	78	-24529.0150	79	657.9359	0.000	0.571480	0.450
ND2	0,0670	-31769.5279		-31502.5684		-31498.5036		533.9191	0.000	-8.129668	**0.004**
ND3	0,0607	-11403.3678		-11183.4729		-11183.4729		439.7899	0.000	0.000010	1.000
ND4	0,0511	-40498.0727		-40032.1913		-40026.0861		931.7628	0.000	-12.210500	**0.000**
ND4L	0,0727	-10118.1495		-10076.4001		-10075.2708		83.4989	0.000	-2.258408	0.133
ND5	0,0676	-51970.2413		-51088.0681		-51092.3346		1764.3464	0.000	8.533012	**0.003**
ND6	0,1009	-16916.1956		-16691.7006		-16691.7006		448.9899	0.000	0.000018	1.000

Degrees of freedom = 1.

[a] A: All branches have one ω; B: All branches have same ω=1; C: Each branch has its own ω.

[b] The natural algorithm of the likelihood value.

[c] Number of parameters.

[d] Bold faced figure indicate the statistical significance ($P < 0.05$).

Table 5(on next page)

Summary of codon model results using the aBSREL approach.

Table 5. Summary of codon model results using the aBSREL approach.

Gene	Number of Selected Branches (P<0.05)	Taxon	ω	Proportion of Codons Under Selection
ATP8	1	*Microceramus pontificus*	288	0.460
COX1	1	*Achatinella mustelina*	2180	0.086
COX3	2	Arionoidea	670	0.053
		Philomycus bilineatus	119	0.092
ND3	1	*Helicella itala*	49.4	0.220
ND4	1	*Succinea putris*	4.18	0.370
ND6	1	*Vertigo pusilla*	15.6	0.370

Table 6(on next page)

Codons under diversifying or positive selection under codon-based models.

Table 6. Codons under diversifying or positive selection under codon-based models.

Gene	BEB	FUBAR	MEME
ATP6	-	4	44
ATP8	-	44	44, 57, 64, 92, 109
COX1	-	-	-
COX2	-	32	-
COX3	-	-	-
CYTB	-	12	12
ND1	-	-	-
ND2	188	-	14, 16, 174
ND3	-	-	27
ND4	109, 170, 192, 301, 386, 427	-	9, 99
ND4L	-	13, 57	13, 57, 109, 111
ND5	451	-	260, 501
ND6	-	-	109, 179, 183